Institute of Biotechnology – Helsinki Institute of Life Science
Cell and tissue dynamics research program
Doctoral Programme in Integrative Life Science
Faculty of Biological and Environmental Sciences
University of Helsinki

Molecular and Cellular Basis of Early Development of the Mammary Gland

Ewelina Trela

ACADEMIC DISSERTATION

To be presented for public examination with the permission of
the Faculty of Biological and Environmental Sciences of the University of Helsinki
in room 1015, Biocentre 2 (Viikinkaari 5, Helsinki) on the 23rd of September 2021,
at 12 o'clock.

Helsinki 2021

Supervisor	Docent Marja Mikkola University of Helsinki, Finland
Advisory committee	Docent Satu Kuure University of Helsinki, Finland and Professor Juha Klefström University of Helsinki, Finland
Pre-examiners	Adjunct Professor Emilia Peuhu University of Turku and Professor Aki Manninen University of Oulu
Opponent	Associate Professor Renée van Amerongen University of Amsterdam
Custodian	Professor Juha Partanen University of Helsinki, Finland

Cover image: 3D surface rendering of a mammary gland (cyan) at embryonic day 13.5 and epidermis (green) filtered with accented edges in Adobe Systems Photoshop 2021.

The Faculty of Biological and Environmental Sciences uses the Urkund system (plagiarism recognition) to examine all doctoral dissertations.

Published in Dissertationes Scholae Doctoralis Ad Sanitatem Investigandam Universitatis Helsinkiensis

ISBN 978-951-51-7479-6 (paperback)
ISBN 978-951-51-7480-2 (PDF)
ISSN 2342-3161 (print)
ISSN 2342-317X (online)
http://ethesis.helsinki.fi

Cover Layout: Anita Tienhaara
Layout: Tinde Päivärinta/PSWFolders Oy/Ltd
Printed by: Painosalama Oy 2021
Helsinki 2021

You cannot hope to build a better world without improving the individuals. To that end each of us must work for his own improvement, and at the same time share a general responsibility for all humanity, our particular duty being to aid those to whom we think we can be most useful.

~ Maria Skłodowska-Curie

TABLE OF CONTENTS

LIST OF ORIGINAL PUBLICATIONS VI

ABBREVIATIONS VII

ABSTRACT IX

1. REVIEW OF THE LITERATURE 1

- 1.1. INTRODUCTION TO MAMMARY GLAND 1
  - 1.1.1. The origin of the mammary gland 1
  - 1.1.2. Mammary gland across mammals (monotremes, marsupial, and placental mammals) 1
- 1.2. ECTODERMAL ORGANS 2
  - 1.2.1. Mammary gland as an ectodermal organ 3
  - 1.2.2. Epithelial morphogenesis 3
  - 1.2.3. Actomyosin network in epithelial morphogenesis 4
  - 1.2.4. Epithelial-mesenchymal interactions in ectodermal appendage morphogenesis 5
- 1.3. MAMMARY GLAND DEVELOPMENT 6
  - 1.3.1. Embryonic mammary gland development 6
  - 1.3.2. Postnatal mammary gland development, molecular regulation, and homeostasis 10
  - 1.3.3. Molecular regulation of embryonic mammary gland development 12
    - 1.3.3.1. Overview of signaling pathways involved in early mammary morphogenesis 13
    - 1.3.3.2. Ectodysplasin/NF-κB pathway 15
    - 1.3.3.3. From mammary line to buds 17
    - 1.3.3.4. From buds to branches 20
  - 1.3.4. Cellular mechanisms driving embryonic mammary gland development 21
  - 1.3.5. Implications of embryonic mammary gland studies in breast cancer 22

2. AIMS OF THE STUDY 24

3. MATERIAL AND METHODS 25

4. RESULTS AND DISCUSSION 28

- 4.1. DOWNSTREAM TARGET GENES OF EDA/NF-κB IN MAMMARY RUDIMENTS (I, II) 28
- 4.2. EDA/NF-κB TARGET GENE FGF20 REGULATES MAMMARY BUD SIZE (II) 29
- 4.3. FORMATION OF EDA/NF-κB INDUCED ECTOPIC MAMMARY PLACODES IS WNT DEPENDENT (I) 32

4.4. ECTODERMAL CELL HYPERTROPHY AND CELL PROLIFERATION HAVE MINOR CONTRIBUTION IN EARLY MAMMARY RUDIMENT DEVELOPMENT (III) 33
4.5. CELL MIGRATION FUELS CELL INFLUX THAT DRIVES EARLY MAMMARY RUDIMENT FORMATION (III) 35
4.6. EDA/NF-κB PATHWAY HAS MINOR INFLUENCE ON CELL PROLIFERATION DURING MAMMARY RUDIMENT FORMATION (UNPUBLISHED) 37
4.7. EPIDERMAL KERATINOCYTES, RING CELLS, MEDIATE MAMMARY BUD INVAGINATION THROUGH ACTOMYOSIN CONTRACTILITY (III) 39

5. CONCLUDING REMARKS AND FUTURE PROSPECTIVES 44

ACKNOWLEDGEMENTS 45

REFERENCES 47

LIST OF ORIGINAL PUBLICATIONS

The thesis is based on original publications, which in the text are referred to by their Roman numerals.

I Voutilainen M, Lindfors PH*, **Trela E***, Lönnblad D, Shirokova V, Elo T, Rysti E, Schmidt-Ullrich R, Schneider P, Mikkola ML, Ectodysplasin/NF-κB Promotes Mammary Cell Fate via Wnt/-catenin Pathway. PLoS Genet, 2015; 11: e1005676. * equal contribution

II Elo T, Lindfors PH, Lan Q, Voutilainen M, **Trela E**, Ohlsson C, Huh SH, Ornitz DM, Poutanen M, Howard BA, Mikkola ML, Ectodysplasin target gene Fgf20 regulates mammary bud growth and ductal invasion and branching during puberty. Sci Rep, 2017; 7(1):5049.

III **Trela E**, Lan Q, Myllymäki SM, Villeneuve C, Lindström R, Kumar V, Wickström SA, Mikkola ML, Cell influx and contractile actomyosin force drive mammary bud growth and invagination. J Cell Biol, 2021; 220 (8): e202008062.

Contributions:

I E.T. participated in the experimental design for the study, carried out experiments and analyzed the data for Fig. 6, Fig. 7, and was responsible for performing experiments for manuscript revision.

II E.T. performed experiments requested in the manuscript revision including RNA *in situ* hybridizations and immunostaining of Lef1 (Fig. S2).

III E.T. conceptualized the study together with the supervisor, carried out all the experiments and data collection. Additionally, E.T. found and validated proper image analysis methods and performed most of data analyses. E.T. wrote the first draft of the manuscript and finalized it together with the supervisor.

ABBREVIATIONS

AD	Autosomal dominant
APC	Adenomatous polyposis coli
AR	Autosomal recessive
Areg	Amphiregulin
Bmp	Bone morphogenetic protein
BrdU	5-bromo-2’-deoxyuridine
CK1	Casein kinase 1
Dhh	Desert hedgehog
Dkk	Dickkopf family proteins
E	Embryonic day
ED	Ectodermal dysplasia
Eda	Ectodysplasin
Edar	Eda receptor
Egf	Epidermal growth factor
Egfr	Epidermal growth factor receptor
Epr	Epiregulin
Fgf	Fibroblast growth factor
Fgfr	Fibroblast growth factor receptor
Fzd	Frizzled, transmembrane receptor
Ghr	Growth hormone receptor
Gli	Glioma-associated oncogene
GSK3β	Glycogen synthase kinase 3 β
HED	Hypohidrotic ectodermal dysplasia
Hh	Hedgehog pathway
Igf1	Insulin-like growth factor 1
Ihh	Indian hedgehog
ISH	In situ hybridization
Lgr	Lecuine-rich repeat-containing G-protein-coupled receptors
Lrp5/6	Low density lipoprotein related proteins 5 or 6
NMII	Non-muscle myosin II
Nrg	Neuregulin
mAG1	monomeric Azami Green
mKO2	monomeric Kuzabi Orange
pMLC	Phosphorylated myosin light chain
PTH	Parathyroid hormone
PTHrP	Parathyroid hormone related protein
PTHR1	Parathyroid hormone/Parathyroid hormone related protein receptor
qRT-PCR	quantitative real-time reverse-transcriptase-PCR
Rspo	R-spondin family

Shh	Sonic hedgehog
Smo	Smoothened
TEBs	Terminal end buds
Tgfα	Transforming growth factor alpha
Tgfβ	Transforming growth factor beta
TNF	Tumor necrosis factor
TNFR	Tumor necrosis factor receptor
Wnt	Wingless-related integration site, Wnt signaling family member
XL	X-linked
^{3}H-TdR	Tritiated thymidine

ABSTRACT

The mammary gland, a specialized organ providing nutrition for mammalian offspring, commences during embryogenesis with the formation of an epithelial thickening known as, placode. Subsequently, the placode enlarges creating a hillock and invaginates into underlying mesenchyme, marking the transition to a bulb stage. By the time of birth, the primary rudimentary ductal tree forms through branching morphogenesis. The development of the organ continues postnatally, and its full maturation is accomplished during pregnancy and lactation. Signaling pathways involved in mammogenesis are well characterized. Among them ectodysplasin (Eda) is key regulator of ectodermal appendages formation in all vertebrates. Eda belongs to tumor necrosis factor family and mediates signaling through transcription factor NF-κB. In humans, mutations in Eda or other components of this signaling pathway lead to hypohidrotic ectodermal dysplasia (HED), characterized by sparse hair, missing teeth, and defects in several exocrine glands including the breast. Mice overexpressing Eda (*K14-Eda*) exhibit supernumerary mammary glands and a hyperbranching phenotype. Despite growing knowledge on molecular signaling regulating mammogenesis, cellular mechanisms are still poorly characterized. The aim of this thesis work was to uncover how Eda regulates mammary gland development and to identify the key cellular mechanisms driving mammary bud formation.

In this thesis work, molecular and cellular mechanisms of early mammary gland development were studied. The transcriptional target genes of Eda were identified, among them members of Wnt, Fgf, TNF, Tgfß, chemokine and Hh signaling pathways. It was shown that in *K14-Eda* mice supernumerary glands also formed in the neck region, whereas formation of ectopic mammary placodes on the flank was mediated through Eda-dependent Wnt pathway upregulation. Using the *Fgf20 null* mouse model the role of Eda target gene, *Fgf20* in mammogenesis was studied. Results showed that while Fgf20 is dispensable for mammary placode formation, its depletion led to the bud size defect. Cellular mechanisms driving early mammary primordium development were elucidated using 3D and 4D confocal microscopy. It was shown that early mammary rudiment growth is predominantly mediated through migration-driven cell influx, with cell hypertrophy and cell proliferation making minor contributions in this process. Additionally, cell migration in the mammary placode stage was documented by live imaging for the first time. The invagination of the mammary bud was shown to be mediated through contractile rim of epidermal keratinocytes adjacent to the bud, named ring cells. Conditional deletion of *Myh9*, encoding heavy chain of non-muscle myosin IIA, led to decreased actomyosin network and a compromised ring cell shape indicative of their impaired function. In addition, abnormal mammary bud shape and defective invagination was observed suggesting an essential role of NMIIA in this process.

1. REVIEW OF THE LITERATURE

1.1. INTRODUCTION TO MAMMARY GLAND

In 1758 Carolus Linnaeus, a renowned taxonomist classified all animals bearing characteristic mammae, or mammary glands, into one group: Mammalia (Gregory, 1910, Linné, 1789). The Mammalia group represents a diverse collection of animals, large and small, arctic and tropical, social and solitary, that all base their life history strategy on a dependency on milk as a source of nutrition for the offspring. The composition of milk varies greatly among mammals and contains proteins that are not found elsewhere in nature (Oftedal, 2012). These unique secretions are produced by a specialized exocrine organ, the mammary gland, that has fascinated scientists for centuries.

1.1.1. The origin of the mammary gland

The group Mammalia consists of the three taxonomic clades monotremes (platypus and echidnas), metatherians (marsupials) and eutherians (placental mammals) that evolved from synapsids, the lineage ancestral to mammals (Oftedal, 2002). This common ancestor laid permeable, parchment-shelled eggs similar to the ones of living monotremes. The parchment-like shells of early synapsids were desiccation intolerant, relying on supplemented water for completion of egg development. The secretion from apocrine-like glands evolved to provide both the required water and the innate immune system for skin and egg protection, marking the evolution of lactation. This ancestral apocrine-like gland combined multiple modes of secretion and was associated with hair follicles and sebaceous glands (pilosebaceous unit). Although not identical, the mammary gland and apocrine gland of mammalian integument possess many similarities. They both have a bilayered secretory portion and, during development, penetrate deep into the hypodermis. Active secretion of the glands is achieved under hormonal stimulation during puberty and in some mammalian taxa there is a transitory or permanent association with hair follicles and sebaceous glands (Oftedal, 2002). The nutritional needs of growing offspring are immense. This, combined with the difficulty associated with catching and digesting the complex meals of adult mammals, shows the evolutionary basis for milk dependency and how its development was key in the success of mammals (Pond, 1977).

1.1.2. Mammary gland across mammals (monotremes, marsupial, and placental mammals)

The extant monotremes are egg-laying mammals. Mammary gland development in these animals is characterized by a plate-like mammary bulb with 100-200 primary sprouts. Each of the sprouts consists of mammary secretory tissue and a pilosebaceous unit. In a mature mammary patch, all the components are fully developed and functional. Interestingly, monotremes do not have a nipple as in other mammals (Oftedal and Dhouailly, 2013). Marsupials early mammary gland is characterized by a single primary sprout per gland.

When both mammary tissue and associated pilosebaceous units are formed the hollowed-out sprout everts forming a nipple. Even though hair follicle and sebaceous glands undergo maturation, the mammary gland associated hairs are shed prior to nipple eversion. The fully formed mammary gland consists of many mammary gland's ductal/secretory tissues and associated pilosebaceous units that drain to one nipple (Oftedal and Dhouailly, 2013). Mammary gland development in placental mammals is characterized by one or many sprouts per gland and are not associated with hair follicles, as this was lost during evolution (Oftedal and Dhouailly, 2013).

1.2. ECTODERMAL ORGANS

The surface of a developing vertebrate embryo is covered by a single layered sheet of cells originating from ectoderm. Due to their tightly bound nature, they are referred to as epithelial cells. The single layered ectodermal cells are covered by protective layer of periderm that will be shed during the course of development and the ectodermal layer will stratify to become cornified outer tissue, the epidermis (M'boneko and Merker, 1988, Richardson et al., 2014). It is the largest organ in the body and functions as a protective shield separating two different chemical milieus. Its impressive performance is achieved by certain cells' characteristics and a variety of ectodermal-derived organs. During development subsets of ectodermal cells will undergo reciprocal interactions with underlying mesenchyme leading to the formation of variety of accessory structures, the ectodermal organs. These include hair, teeth, feathers, scales, beaks, horns, nails, as well as several exocrine glands including salivary, sweat, lacrimal and mammary glands. The organogenesis of this group of derivatives with wide functional range, form and shape, is initiated during embryogenesis while full organ maturity is achieved postnatally.

The location and onset of development differs among ectodermal organs, yet they share several similarities in their morphogenesis. They have a common origin which consists of two layers, one ectodermal and one mesenchymal, and proceed through similar morphological stages until they reach the bud stage, upon which they diverge to continue on their individual developmental path (Biggs and Mikkola, 2014). The first visible sign of organogenesis is the formation of a thickened cluster of ectodermal cells called placode, which in the mammary gland appears as truly stratified structure. Subsequently, ectodermal organs progress into bud stage and undergo characteristic folding into (invagination as in mammary gland) or out (evagination as in feather) of mesenchymal tissue. From this stage onwards each organ continues diversification through specific patterns of epithelial growth associated with folding and/or branching that ultimately results in the final organ (Pispa and Thesleff, 2003).

Genetic regulation of these early developmental stages is conserved across species and shared between ectodermal organs (Chuong, 1998, Pispa and Thesleff, 2003, Mikkola and Millar, 2006). Mutation in one gene regulating development of the ectodermal organs may lead to condition where the phenotype is visible in several cutaneous structures known as ectodermal dysplasias (EDs). This large group of congenital hereditary disorders is characterized by the abnormalities in the development of at least two epithelial structures (e.g. hair, tooth, sweat or mammary gland) (Itin and Fistarol, 2004, Reyes-Reali et al., 2018).

1.2.1. Mammary gland as an ectodermal organ

Unlike most ectodermal organs, mammary gland development involves two different mesenchymal tissues, namely mammary mesenchyme (a.k.a. primary mammary mesenchyme) and mammary fat pad tissue (Sakakura et al., 1982). Mammary mesenchyme consists of connective tissue located in immediate vicinity to the mammary rudiment. The fat pad tissue localizes posterior to the mammary primordium and in adult mice is comprised of various cell types including adipocytes, a few interspersed fibroblasts, and vascular and immune cells (Inman et al., 2015). The fat pad is thought to differentiate from subcutaneous mesenchymal cells independently of mammary mesenchyme (Sakakura et al., 1982). These two types of mesenchymal tissue play crucial roles in different developmental stages of the embryonic mammary gland: the mammary mesenchyme during early and the fat pad tissue during late embryonic development.

1.2.2. Epithelial morphogenesis

Morphogenesis is a complex developmental process during which multiple cells receive and respond to both molecular and mechanistic cues which culminate in the final organ. Therefore, morphogenesis requires, the appropriate cells to be specified and undergo the appropriate cell behaviors (Pilot and Lecuit, 2005). Several types of cell specification are known, and each is achieved through a distinct morphogenetic stimuli (Gilbert, 2014). Among them Wolpert's positional information model (Wolpert, 1969, Wolpert, 1971) and Turing's reaction-diffusion model (Turing, 1952). The well-recognized positional information model assumes that morphogen gradient drives cell specification according to the cell's position within a chemical or mechanical gradient. This type of cell specification was shown in the segmented body plan of *Drosophila* where the identity of each segment is defined by *pair-rule* gene expression based on priori established anterior-posterior gradient of *bicoid* gene expression (Driever and Nusslein-Volhard, 1988, Nusslein-Volhard and Wieschaus, 1980, Riddihough and Ish-Horowicz, 1991, Small et al., 1991). The reaction-diffusion model assumes that cells produce two morphogens that are characterized by different rates of diffusion where one acts as an activator and the other as an inhibitor. The activator induces its own production and that of the inhibitor and is defined by diffusion that operates locally whereas the inhibitor diffuses quickly and acts over a limited distance. This interplay leads to the generation of the tissue pattern, which has been shown in patterning of mouse hair follicles (Sick et al., 2006).

Tissue type involved in morphogenesis and said tissue's inherent characteristics, play a crucial role as the cell responds to morphogenetic stimuli including changes in the cell architecture and/or polarity. Ectodermal epithelium is a coherent, tightly connected sheet of cells with well-defined apical (facing the external environment or luminal space in case of the internal epithelia) and basal (facing the internal body environment) polarity residing on the thin basement membrane. Despite tightly connected cells, epithelial tissues are dynamic and may undergo distinctive shape changes that involve invagination (folding inwards), evagination (folding outwards), elongation, bending, and separation of epithelial cell sheets (Lecuit et al., 2011, Heisenberg and Bellaiche, 2013, Guillot and Lecuit, 2013, Pilot and Lecuit, 2005). The final organ shape and development of sophisticated structures such as the mammary gland are formed as a consequence of epithelial tissue morphogenesis. The successful shaping of any ectodermal derivative requires organized and coordinated cellular responses which include cell division, cell death, cell migration, cell growth and cell shape changes (Lecuit and Lenne, 2007). Current understanding of such cellular mechanisms come mainly from studies in *Drosophila melanogaster* and *Xenopus laevis*. Processes such as apical constriction, in which a cell's apical domains shrink while the volume remains rather stable, or convergent extension, that leads to tissue elongation, have been found and explained using these model organisms and remain relevant to mammalian development as well (Perez-Vale and Peifer, 2020, Shindo, 2018). Moreover, these studies also underline the importance of actomyosin contractile network in epithelial morphogenesis.

1.2.3. Actomyosin network in epithelial morphogenesis

The cytoskeleton is responsible for providing cell shape, a scaffolding for transportation within the cell, and a mechanism for mechanical force production, all of which are required for morphogenesis (Hohmann and Dehghani, 2019). Part of the cytoskeleton in eukaryotic cells consists of actin-based microfilaments and associated actin-binding proteins which encapsulate the cell, creating a network that is bound to the plasma membrane known as the cell cortex (Chugh and Paluch, 2018). One example of actin-binding proteins are non-muscle myosin II (NMII) proteins functioning as motor proteins that act on filamentous actin network leading to filament sliding and generation of contractile force.

Contractile elements consisting of actin, NMIIs, and various crosslinking proteins are termed stress fibers and give rise to cortical tension (Lehtimaki et al., 2017). Coupling of stress fibers to the extracellular matrix through focal adhesions allows cells to sense and respond to the extracellular environment and play a key role in cellular mechanics and force sensing. Dynamic mechanics of stress fibers assembly is controlled both at focal adhesions and along the stress fibers themselves by vast numbers of actin- and myosin-binding proteins. The activity of these proteins is controlled by mechanical forces and various signaling molecules among which the RhoA family of small GTPases is considered the master regulator (Lehtimaki et al., 2017).

Actin-binding NMIIs form hexamers consisting of two heavy chains, two regulatory light chains and two essential light chains. The activity of NMII is regulated through dynamic phosphorylation and dephosphorylation of the regulatory light chain (Munjal and Lecuit, 2014). There are three NMII heavy chain isoforms, *Myh9* (NMIIA), *Myh10* (NMIIB), and *Myh14* (NMIIC) that fold into a globular head domain responsible for mediating motor activity. All these heavy chains have been shown to localize to the cortex (Chugh and Paluch, 2018). NMIIs are expressed in wide variety of tissues however some of them are predominant in certain cell types: NMIIA is most abundantly expressed in epithelial and endothelial cells and NMIIB in cardiac muscle (Ma et al., 2010, Shutova and Svitkina, 2018). The exact role and expression pattern of NMIIC remains poorly understood (Shutova and Svitkina, 2018). Interestingly, different NMII isoforms can co-assemble into mixed minifilaments, however, whether they exert distinct function in the cortex remains unknown (Beach et al., 2014, Shutova et al., 2014).

A well-studied example showing the crucial role of the actomyosin network and actin cortex in epithelial morphogenesis is apical constriction (Gillard and Roper, 2020). This mechanism is defined as the shrinkage of the apical side of an epithelial cell leading to cell shape change from columnar or cuboidal to trapezoidal, wedge-shaped or bottle-shaped. Resulting apical constriction can have different outcomes on tissue geometry depending on the physiological context (Martin and Goldstein, 2014). For cell shape change, the actomyosin network must be coupled to adherens junctions. It has been established that there are a variety of ways in which actomyosin dynamics and adherens junctions are regulated during apical constriction. Depending on the position of the actomyosin network and fibers (circumferential versus medioapical), their dynamics (pulsing vs continuous), potency of coupling to adherens junctions (weak versus strong) and maintenance of apical cell shape between contractile events have outcome in different forms of apical constriction that are brought about e.g., tissue bending or individual cell ingression. This suggests that the ‘molecular engine’ can be organized in a specific way leading to the outcome that fits a specific morphogenetic process.

Despite long standing fascination of cellular mechanisms driving morphogenesis, availability of limited resources in microscopy techniques have restricted progress in this field in mammalian systems. Bursts in recent advances in confocal microscopy together with development of light sheet fluorescent microscopy, suitable for larger specimens, sparked recurring interest. This opens up the way for new discoveries of cellular mechanisms in stratified tissues which still largely remain unexplored.

1.2.4. Epithelial-mesenchymal interactions in ectodermal appendage morphogenesis

In the context of ectodermal organ morphogenesis, epithelial and mesenchymal compartments and their reciprocal interactions play a crucial role in this process. The continuous crosstalk between the epithelium and the mesenchyme is fundamental for the proper appendage function but more importantly it is essential for the induction of ectodermal organ development. Even though the epithelium originates from ectoderm, the source of the mesenchymal compartment differs among organs. Trunk hair and mammary gland mesenchyme stems from mesoderm whereas tooth, vibrissae, and cranial hair is from the neural crest (Mikkola, 2007). For some ectodermal organs, elegant tissue recombination studies have led to the identification of the source of the inductive signals. In this type of experiment, the epithelial and mesenchymal compartment is separated by enzymatic treatment and can be recombined with tissues of diverse age, body location and source (species) (Sengel, 1976, Parmar and Cunha, 2004). Tissue recombination led to the establishment that for hair follicle the inductive signal emerges from mesenchyme, whereas for tooth initial inductive potential resides in epithelium, and later shifts to the mesenchyme (Biggs and Mikkola, 2014).

1.3. MAMMARY GLAND DEVELOPMENT

The mammary gland is a very dynamic organ whose structure changes through the life of a female under the influence of the reproductive cycle. Development of the mammary gland can be divided into embryonic and postnatal stages. While embryonic and prepubertal stages are unaffected by hormonal cues, postnatal gland maturation is connected to sexual development and reproduction and can be further broken down to pubertal stage, pregnancy, lactation and involution.

In this thesis mouse was used as a model organism to study mammary gland development. Therefore, subsequent chapters review literature from murine studies. It is worth mentioning that mouse and human mammary gland share similarities but there are significant differences as well including mammary gland architecture, hormonal milieu, and differences in reproductive cycle (for more detail see (Dontu and Ince, 2015, Mcnally and Stein, 2017)).

1.3.1. Embryonic mammary gland development

The embryonic development of mammary gland commences with the formation of the bilateral milk or mammary lines at around embryonic (E) day 10.5 on the dorso-ventral border of mouse embryo flanks between fore and hind limb buds (Fig. 1) (Sakakura, 1987).

In mice, these structures are defined by the expression of several molecular markers belonging to the Wingless-related integration site (Wnt) signaling pathway and appear as a small band of pseudostratified epidermal cells (Chu et al., 2004, Veltmaat et al., 2004, Veltmaat et al., 2006). Interestingly, these Wnt positive streaks emerge as three separate bands, the first the one on the flank between fore and hind limbs followed by additional two in axillary and inguinal region, to only connect with each other later (Veltmaat et al., 2004). In the next 24 hours, milk lines resolve into five pairs of elliptical pseudostratified multilayered placodes, each pair appearing symmetrically, but individual pairs developing in an asynchronous manner (Fig. 2) (Veltmaat et al., 2004, Veltmaat et al., 2003). Placode

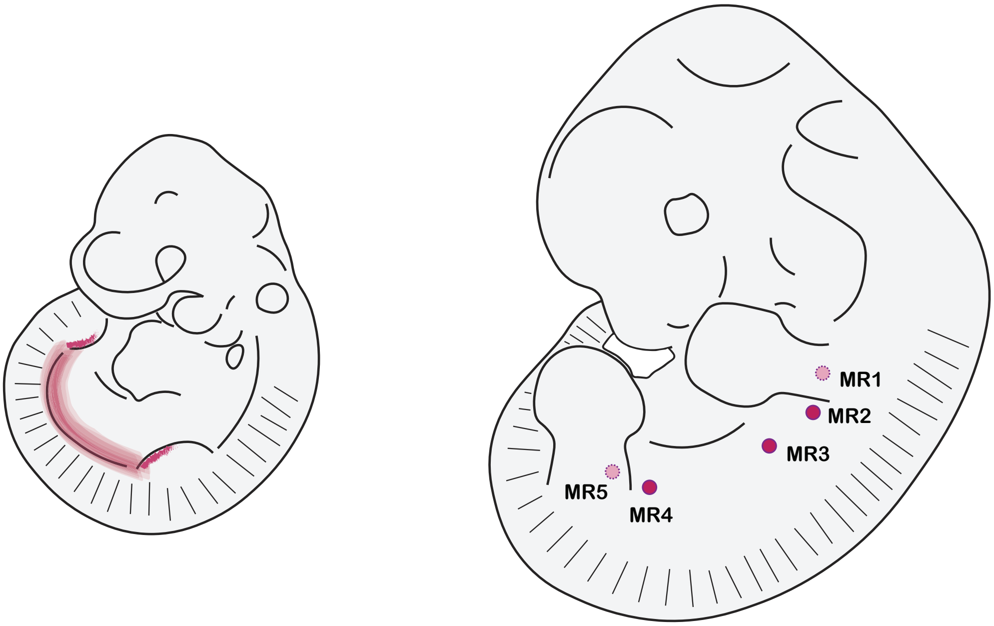

Figure 1. Position of milk line and mammary rudiments in mouse embryo.
Milk line appears as three separate bands of cells expressing Wnt10b marker, first one between fore and hind limbs (▨). Additional two bands appear around fore and hind limbs (▬) slightly later in the development. Milk line resolves into five pairs of mammary rudiments (MR1-5), three in the thoracic region and two in the inguinal region. Mammary rudiment that is covered by limbs is indicated as (◌).

3 is the first morphologically discernible, placode 4 appears subsequently, followed by placodes 1 and 5 that form at the same time. The last placode that develops is placode 2 (Fig. 1) (Veltmaat et al., 2004).

Next, placodes enlarge, accumulating cells which creates mammary hillock that is elevated above the surface of the surrounding epidermis at E12.5 (Fig. 2). Hillocks are morphologically visible as prominent knobs on the mouse embryo flanks (Chu et al., 2004, Veltmaat et al., 2004). This developmental stage also marks the induction of the invagination process in which the mammary hillock starts sinking into the underlaying mammary mesenchyme that undergoes dramatic changes at this time (Sakakura, 1987, Sakakura et al., 1982).

Mesenchymal cells start to elongate and orient concentrically around the mammary rudiment generating several layers of condensed mesenchyme. Subsequently, at E13.0, the hillock transforms into a spherical structure, referred to as a mammary bud (Fig. 2) (Propper et al., 2013). Around the same time, the epidermis starts differentiation indicated by the generation of a suprabasal layer on top of the basal layer. At E13.5, mammary primordium

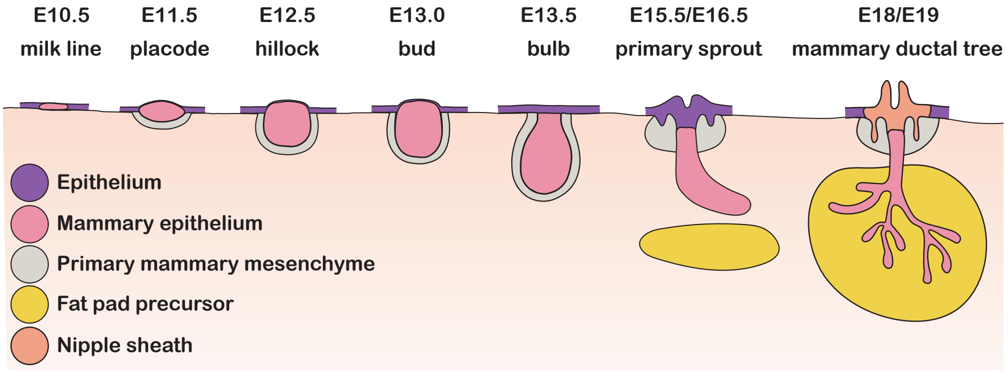

Figure 2. Schematic representation of embryonic mammary gland development in mice. *Embryonic mammary gland development commences with the formation of milk line at E10.5 that subsequently resolves into epithelial thickening known as placode. By E12.5 placode enlarges creating hillock followed by bud and bulb stages. Primary mammary sprout forms by E15.5/E16.5 and grows downwards toward fat pad precursor tissue. By E18/E19 mammary ductal tree with 10 to 15 branches develops.*

sinks deeper and becomes surrounded by the mammary mesenchyme. This stage is marked by the formation of the constricted neck region connected to the epidermis. Due to resemblance of a light bulb, mammary rudiment at this developmental stage is referred as a bulb (Fig. 2). Stages between E14.0 and E15.5 are regarded as relatively quiescent in female mice, however, at this time, posteriorly to mammary rudiment a secondary mammary mesenchyme, the precursor of the fat pad starts to emerge around E14.0 (Sakakura et al., 1982). While the fat pad continues to develop, mammary primordium at around E15.5 enters the sprout stage in which the distal end of the bulb elongates and grows downwards into the fat pad tissue (Fig. 2). In this new adipocytic environment, mammary rudiment begins branching morphogenesis around E16.5 through a series of ramifications. By E18.5, a small primary mammary tree with 10 to 15 branches and a primary duct is formed.

Prior to birth, two important morphological processes take place. The formation of the lumen is initiated and epidermal cells overlying mammary primordium are remodeled into the typical nipple structure (Hogg et al., 1983, Foley et al., 2001). Development of the nipple requires inhibition of hair follicle formation, thickening of epidermis in close vicinity to the mammary rudiment and proper epidermal folding in an umbrella-like fashion in order to create a ridge that will encircle the primary epithelial duct (Fig. 2). By the end of embryonic mammary gland development, the ductal tree of mammary rudiment is formed, and mammary mesenchyme is remodeled into dense connective tissue associated with the nipple sheath.

Importance of epithelial-mesenchymal interactions in embryonic mammary gland development

The influence of mesenchymal environment and reciprocal interactions between epithelial and mesenchymal compartments in mammary gland morphogenesis is essential. This idea was established through a series of tissue recombination experiments. Elegant work done by Propper and colleagues indicated that the condensed primary mammary mesenchyme bears inductive signal that instructs the overlaying ectoderm to form a mammary rudiment (Propper, 1968, Propper and Gomot, 1967, Propper and Gomot, 1973). They showed that when E13.0 rabbit mammary mesenchyme was recombined with E6.0 chick ectoderm, mammary gland-like structures were induced. Later this was confirmed by studies showing that mammary primordia fail to develop in the absence of the mammary specific mesenchyme (Kratochwil, 1969). Another body of evidence showed that upon recombination of E13.0 mouse mammary mesenchyme with E13.0 rat epidermis and grafting *in vivo*, the mammary rudiment that formed expressed mammary specific markers (Cunha et al., 1995). All these studies established that the primary mammary mesenchyme induces and specifies epidermal cells into the mammary epithelial path, both morphologically and functionally. Experiments in which E14.0 salivary gland mesenchyme was combined with E16.0 mammary gland epithelium and grown under kidney capsules showed that the resulting branched organ resembled the salivary gland. However, epithelium exhibited cytodifferentiation specific for mammary epithelium. This result indicated that mesenchyme governed branching pattern, still the mammary cell fate was retained (Sakakura et al., 1976).

Epithelial-mesenchymal interactions are important not only for induction of mammogenesis and mammary epithelium specification but play a crucial role in establishing sexual dimorphism of mammary gland in mouse embryos. Until E14.0 female and male mammary gland development proceeds similarly (Veltmaat et al., 2003). Starting from E13.5, after sex-specific differentiation of the gonads, the mammary mesenchyme around the neck of the bulb in male embryos starts to aggregate. Condensation of the mesenchyme leads to the disconnection of the bulb from the overlying epidermis and both mammary mesenchyme and mammary epithelium undergo apoptosis. This destruction of the mammary gland was shown to be mediated through testosterone-activated androgen receptor present in mammary mesenchyme (Dunbar et al., 1999, Heuberger et al., 1982, Kratochwil, 1977). This was later confirmed by studies which reported that male embryos lacking androgen receptor expression developed normal mammary glands and nipples (Kratochwil and Schwartz, 1976, Drews and Drews, 1977). These studies demonstrated also that it is the mesenchyme that responses to testosterone as recombination of androgen-insensitive mesenchyme with wild type epithelium cultured in presence of testosterone resulted in normal mammary gland development. In wild type male embryos, once the mammary bulb is disconnected from the epidermis, the rudiment may completely disappear or persist as a blind duct.

1.3.2. Postnatal mammary gland development, molecular regulation, and homeostasis

In this thesis work I have studied embryonic mammary gland development; therefore, postnatal stages and their molecular regulation will be discussed only briefly.

At birth, the mammary gland consists of a small ductal tree with one primary duct, reaching out into the nipple sheath, embedded on one side of the fat pad tissue (Fig. 3). Until puberty, the gland remains relatively quiescent, undergoing solely allometric growth to keep up with overall body size development (Macias and Hinck, 2012). The adult gland of virgin mice consists of the mammary bilayer composed of apically oriented luminal epithelial cells lining the duct and basally oriented myoepithelial cells in contact with the basement membrane (Inman et al., 2015). In mice luminal cells are characterized by the expression of keratins 8 and 18, whereas myoepithelial cells express keratins 5 and 14.

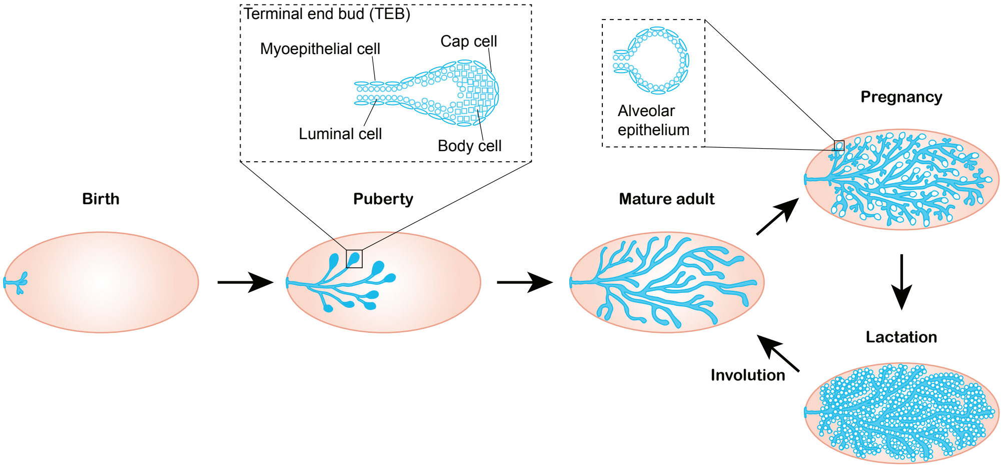

Figure 3. Schematic representation of postnatal mammary gland development.
During prepubertal stages mammary gland remains relatively quiescent until puberty where under hormonal regulation terminal end buds (TEBs) consisting of cap and body cells (giving rise to myoepithelial and luminal cells, respectively) appear and drive ductal elongation filling the fat pad tissue. Mature adult mammary gland responses to hormonal cues upon pregnancy and undergoes structural changes including appearance of alveolar units. Full mammary gland maturation is achieved during lactation. In the absence of milk production promoting stimuli mammary gland undergoes involution to virgin-like state.

Although embryonic and prepubertal mammary gland development is hormone-independent, pubertal stages rely on hormonal input. Hormones such as estrogen, progesterone, prolactin, and growth hormone are key regulators during postnatal mammary gland growth (Macias and Hinck, 2012). The effects of the hormones are mediated by locally produced paracrine factors.

The onset of puberty in mice begins at approximately 3 weeks of age and is characterized by rise in the levels of estrogen and production of growth hormone by the pituitary gland (Prevot, 2015). Estrogen is a membrane-soluble ligand produced by ovaries that activates gene expression through its main receptor, estrogen receptor alpha (ERα) mediating its essential role of proliferation during mammary gland ductal elongation. Secreted growth hormone signals through growth hormone receptor (Ghr) and stimulates the production of insulin-like growth factor 1 (Igf1) in the mammary stroma. As a result Igf1 promotes the formation of terminal end buds (TEBs), club-shaped structures located at the tips of the elongating ducts, that emerge at the onset of puberty (Fig. 3) (Williams and Daniel, 1983, Gallego et al., 2001, Ruan and Kleinberg, 1999).

TEBs consist of two cell types, inner layer of body cells enveloped by a single layer of cap cells (Fig. 3) that give rise to luminal and myoepithelial cells, respectively (Heisenberg and Bellaiche, 2013, Williams and Daniel, 1983). The majority of proliferation takes place in TEBs, and extensive proliferation of the glandular epithelium leads to the growth of the primary ductal tree and complete filling of the fat pad via branching morphogenesis (Fig. 3). Binding of estrogen to a subset of luminal cells leads to the production of amphiregulin (Areg) and activation of epidermal growth factor receptor (Egfr) in a paracrine manner in the stroma. As a result, additional growth factors including fibroblast growth factor (Fgf) are expressed (Paine and Lewis, 2017). Igf1 plays a crucial role in proper branching pattern but is dispensable for TEBs maintenance. Ductal growth ceases once the TEBs reach the edges of the fat pad tissue or are in close proximity with another branch, which as a consequence leads to their regression (Faulkin and Deome, 1960). Additional rounds of branching that is not driven by TEBs, occurs in each estrous cycle in response to progesterone signaling in preparation for a potential pregnancy. If no pregnancy occurs, these structures regress and branch anew in the next estrous cycle (Macias and Hinck, 2012).

The mammary gland undergoes tremendous architecture transformation and remodeling upon pregnancy largely due to progesterone and prolactin (Brisken, 2002). Produced by the ovaries, progesterone, binds to its receptor, PR, leading to activation of target genes, namely receptor activator of nuclear factor κ B ligand (*RANKL*) and *Wnt4* (Rajaram et al., 2015). In turn, RANKL induces proliferation and secretory fate in neighboring cells in paracrine fashion. Progesterone together with prolactin promote extensive proliferation and differentiation of specialized and complex structures called alveolar units consisting of alveolar cells (Fig. 3). In late pregnancy, these units undergo terminal differentiation into specialized secretory lobules that start to synthesize milk proteins and cytoplasmic lipid droplets.

Secretion of milk does not occur yet, but it is stored in luminal epithelial cells. At birth, levels of progesterone drop precipitously and suckling by the pup causes release of oxytocin. This in turn leads to the contraction of myoepithelial cells surrounding alveoli and movement of the milk through the ductal tree to the nipple, a process known as lactation (Fig. 3). Absence of stimuli inducing milk production promote tremendous rounds of mammary gland regression and clearance called involution (Fig. 3). During this process, alveolar epithelial cells disappear through cell death and are removed from the gland by macrophages and a subset of surviving mammary epithelial cells (Kreuzaler et al., 2011, Wang and Scherer, 2019). As a consequence, the mammary epithelial tree returns to the virgin-like state of the gland, although with more branches than before (Watson and Khaled, 2020).

These astonishing changes occurring in each reproductive cycle and pregnancy exhibit enormous plasticity of the gland owing to mammary stem cells. Stem cells are defined as cells with the capacity to self-renew and giving rise to multipotent cells capable to differentiate into cell types present within given tissue or organ (Fu et al., 2020). Existence and concept of stem cells in mammary gland was first identified through transplantation of normal mammary tissue fragments into de-epithelialized (cleared) fat pads of 3-week-old recipient mice (Deome et al., 1959). As a result, ductal outgrowth resembling the structure of normal epithelial tree formed. Since then, it has been established that under homeostatic conditions unipotent mammary stem cells give rise to separate linages of mammary luminal and myoepithelial cells, yet the existence of rare bipotent mammary stem cells have not been excluded in adult individual (Fu et al., 2020, Watson and Khaled, 2020). In contrast, in embryonic stages fetal mammary stem cells have been identified arising in midgestation embryo (Watson and Khaled, 2020). Initially, these fetal mammary stem cells are bipotent and as embryogenesis progresses become lineage restricted, with rare bipotent stem cells remaining after birth.

1.3.3. Molecular regulation of embryonic mammary gland development

Successful organ morphogenesis requires precise orchestration and coordination of cellular behaviors with cell fate specification and differentiation. Cell fates and behaviors are governed by signaling pathways including Wnt, fibroblast growth factor (Fgf), transforming growth factor β (Tgfβ), epidermal growth factor (Egf), hedgehog (Hh), and parathyroid hormone related protein (PTHrP).

In addition to these signaling pathways, homeobox genes encoding for a large family of transcription factors including Hox, Msx, and Pax transcription factors play a role in embryonic mammary gland development. Homeobox genes contain conserved DNA sequence coding DNA-binding domain called, the homeodomain (Duverger and Morasso, 2008, Holland et al., 2007). The homeodomain transcription factors have been implicated in embryonic development including morphogenesis, patterning, and cell differentiation (Duverger and Morasso, 2008, Holland et al., 2007). The transcription factors of Hox family are involved in various signaling pathways such as Wnt and Tgfβ, and regulate processes including proliferation, apoptosis, motility, and differentiation (Yu et al., 2020).

1.3.3.1. Overview of signaling pathways involved in early mammary morphogenesis

Wnt pathway

Wnt pathway signal transduction is initiated upon binding of one of the 19 secreted Wnt ligands (in mice) to a receptor complex (http://wnt.stanford.edu). The receptor complex consists of transmembrane receptor Frizzled (Fzd) family and co-receptor low density lipoprotein related proteins 5 or 6 (Lrp5/6) family (Van Der Wal and Van Amerongen, 2020). The molecular cascade triggered by Wnt proteins is classified into two categories: canonical (β-catenin-dependent) and non-canonical (β-catenin-independent). Although members of non-canonical Wnt pathway are expressed during embryonic mammary gland development, its precise involvement in mammogenesis is uncertain and it will not be discussed here further (Boras-Granic and Hamel, 2013). In canonical Wnt pathway, in the absence of activating ligand, cytoplasmic β-catenin is phosphorylated and targeted for proteasomal degradation by a destruction complex consisting of two scaffolding proteins: tumor suppressors adenomatous polyposis coli (APC) and Axin; and two kinases: casein kinase 1 (CK1) and glycogen synthase kinase 3 β (GSK3β) (Wiese et al., 2018). Activation of Wnt ligand-receptor complex leads to inactivation of the destruction complex through direct interaction of Lrp5/6 with Axin. As a consequence, β-catenin degradation is inhibited which allows its accumulation in cytoplasm, followed by its translocation to nucleus where it binds the T cell factor/lymphoid enhancer factor (TCF/Lef) family of transcription factor and activates its target genes (Van Der Wal and Van Amerongen, 2020). Additional levels of regulation and complexity in canonical Wnt pathway are added with various inhibitor proteins [e.g., Dickkopf family proteins (Dkk)] and agonists (e.g., R-spondins) (Nusse and Clevers, 2017). The R-spondin family (Rspos) comprised of four Rspo proteins (Rspo1-4) acts as ligands for Lecuine-rich repeat-containing G-protein-coupled receptors 4-6 (Lgr4-6) leading to signal enhancement of low dose Wnt (Nusse and Clevers, 2017, Van Der Wal and Van Amerongen, 2020, Wiese et al., 2018).

Fibroblast growth factor pathway

Fibroblast growth factors (Fgfs) are a family of 22 secreted glycoproteins that signal through transmembrane tyrosine kinase receptors (Fgfr1-4). Fgfr1-3 undergo alternative splicing that results in two isoforms (IIIb and IIIc isoforms) exhibiting different ligand specificities (Ornitz and Itoh, 2015). Differing ligand-binding capacities and preferential expression of ligands and receptors in different tissues underlines dozens of possibilities for context dependent function of Fgf pathway (Xie et al., 2020). Activation of the Fgf pathway leads to signal transduction and triggering of several signaling cascades: RAS-mitogen-activated protein kinase (MAPK), phosphatidylinositol 3-kinase (PI3K), signal transducer and activator of transcription (STAT), and phospholipase C-gamma (PLCγ) pathways (Ornitz and Itoh, 2015, Xie et al., 2020).

Transforming growth factor ß pathway

Transforming growth factor β (Tgfβ) superfamily consists of subfamilies among which are Tgfβ family, the bone morphogenetic proteins (Bmps) family, and others including Activin/ Inhibins family. This large superfamily is responsible for a vast array of cellular responses during embryogenesis and adult tissue homeostasis (Mueller and Nickel, 2012, Budi et al., 2017). Tgfβ ligands bind as dimers and activate two different subtypes of transmembrane serine-/threonine kinase receptors, type I and type II, resulting in the formation of a heterotetrametric receptor complex. Stimulated receptor phosphorylates and activates SMAD proteins which are transcription factors leading to regulation of responsive genes (Mueller and Nickel, 2012, Budi et al., 2017). Context-dependent response control cell physiology, proliferation, growth, and direct cell differentiation (Budi et al., 2017).

Epidermal growth factor pathway

The epidermal growth factor (Egf) family of peptide growth factors include Egf itself, amphiregulin (Areg), epiregulin (Epr), and others including transforming growth factor alpha (Tgfα) and neuregulins (Nrgs) (Wilson et al., 2012, Wee and Wang, 2017). This family of ligands signals through members of ErbB family of receptor tyrosine kinases comprising of the epidermal growth factor receptor (EGFR) 1 (EGFR/ErbB1), ErbB2/HER2/Neu, ErbB3/HER3, and ErbB4/HER4. Interestingly, ErbB2/HER2/Neu lacks the capacity to interact with Egf ligands and activity of ErbB3/HER3 is defective. Yet, these two receptors form heterodimeric complexes with other receptors that lead to potent cellular signaling (Wee and Wang, 2017). Stimulation of Egf signaling pathway results in downstream activation of many signaling pathways such as RAS-MAPK, PI3K/AKT/mammalian target of rapamycin (mTOR), Src kinases, and STAT transcription factors (Arteaga and Engelman, 2014).

Hedgehog pathway

Ligands activating the Hedgehog (Hh) signaling pathway include glycoproteins Sonic Hh (Shh), Indian Hh (Ihh) and Desert Hh (Dhh). They signal through Patched 1 and 2 (Ptch1, 2) receptors that in inactivated state act as repressors for Smoothened (Smo) receptor (Hu and Song, 2019, Lee et al., 2016). Release of Smo receptor activates signaling cascade that results in change of balance between activator and repressor forms of glioma-associated oncogene (Gli1-3) transcription factors. Gli1 acts exclusively as an activator, whereas Gli2 and Gli3 are activators in the presence of ligand and act as repressors in the absence of positive Hh signalling. Governing embryonic development by regulating cell division and cell fates, as well as regulation of tissue homeostasis are major processes regulated by Hh signaling (Hu and Song, 2019, Lee et al., 2016).

Parathyroid hormone related protein pathway

The parathyroid hormone related protein (PTHrP) exhibits structural and functional similarities with parathyroid hormone (PTH). Both proteins signal through the same

G-protein coupled receptor, known as the Type 1 PTH/PTHrP receptor (PTHR1) (Sutkeviciute et al., 2019). PTHrP is widely expressed in different type of tissues and its essential role during normal embryonic and postnatal development. Stimulation of PTHrP signaling leads to the downstream activation of many signaling pathways including cyclic adenosine monophosphate (cAMP)/ protein kinase A (PKA), phospholipase C (PLC)/Ca^{2+}/ protein kinase C (PKC), and MAPK (Mccauley and Martin, 2012, Sutkeviciute et al., 2019).

1.3.3.2. Ectodysplasin/NF-κB pathway

Ectodysplasin/NF-κB signaling pathway

The secreted signaling molecule ectodysplasin (Eda) belongs to the tumor necrosis factor (TNF) superfamily. Two distinct Eda isoforms exist as a product of alternative splicing: Eda-A1 (hereafter Eda) and Eda-A2 (Kowalczyk-Quintas and Schneider, 2014). They signal through TNF receptors (TNFRs): the Eda receptor (Edar) and Xedar (a.k.a. Eda2R), respectively. The exact physiological function of Eda-A2/Xedar signaling axis remains poorly understood (Lindfors et al., 2013), therefore, it will not be discussed here further. The activation of Eda signaling pathway begins with Eda binding to the Edar receptor (Fig. 4). This leads to the engagement of the adaptor molecule Edaradd which in turn triggers the downstream signaling cascade through TNFR-associated factor molecule, Traf6 (Fig. 4). As a result, the canonical NF-κB pathway is activated (Mikkola, 2008). While unstimulated, NF-κB protein is bound to IκBα which prevents it from shuffling to the nucleus. Upon Eda binding and Traf6 activation, the IKK complex, consisting of IKKα (IKK1) and IKKβ (IKK2) kinases and a regulatory subunit IKKγ (NEMO), is triggered and as a consequence, phosphorylates IκBα leading to its degradation. Released NF-κB transfers to nucleus where it activates Eda/NF-κB target genes (Fig. 4).

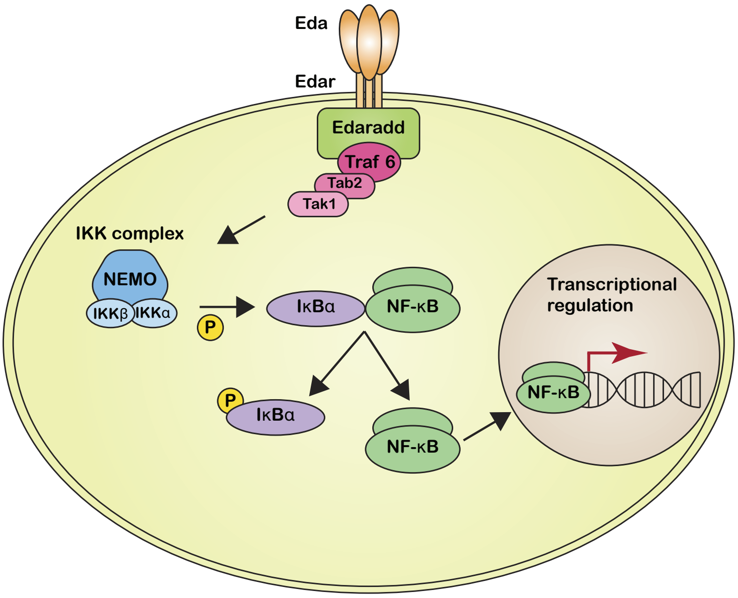

Figure 4. Schematic of Eda/NF-κB signaling pathway. *In the absence of Eda, NF-κB is sequestered by IκBα in the cytoplasm. Upon Eda activation, IκBα is targeted for proteasomal degradation leading to NF-κB release, translocation to nucleus and activation of target genes.*

Hypohidrotic Ectodermal Dysplasia

Hypohidrotic ectodermal dysplasia (HED) is the most common form of EDs. It can be inherited as an X-linked (XL), autosomal recessive (AR), or autosomal dominant (AD) manner (Mikkola, 2009, Wright et al., 2019). Patients affected by HED exhibit missing or poorly developed hair, severe oligodontia, absent or reduced sweating, and defects in many other ectodermal organs. Breast anomalies are also reported in HED patients and include hypoplastic, absent, or supernumerary nipples, and even absence of breast tissue (Clarke et al., 1987, Haghighi et al., 2013, Megarbane et al., 2008). XLHED is caused by mutations in the *Eda* gene (Kere et al., 1996, Srivastava et al., 1997) while AR and AD forms of HED are caused by mutations in *Edar* and *Edaradd* (Bal et al., 2007, Chassaing et al., 2006, Headon et al., 2001, Monreal et al., 1999).

Eda deficient mouse mutants exhibit a phenotype similar to the patients affected by HED. These mice carry mutations in the following genes: *Tabby* mouse (Falconer, 1952, Srivastava et al., 1997) in the *Eda* gene on the X chromosome, *downless* (recessive) and *Sleek* (dominant) mice have *Edar* mutations (Headon and Overbeek, 1999, Majumder et al., 1998), and lastly *crinkled* mouse (Headon et al., 2001, Yan et al., 2002) in *Edaradd* adaptor protein gene. Phenotypes observed in these four mice are similar and include defects in ectodermal organs such as missing or abnormally shaped teeth, abnormal hair composition, missing sweat glands at the footpads, and defective or smaller lacrimal, Meibomian, and submandibular glands.

The importance of Eda/NF-κB signaling pathway in development is also underlined by the fact that it is highly conserved from fish to man and mutations lead to the phenotypic disease affecting organogenesis of many ectodermal organs (Sadier et al., 2014).

Ectodysplasin gain-of-function mouse models

Gain-of-function mouse models in which specific components of Eda/NF-κB pathway are overexpressed have been generated (Mustonen et al., 2003, Pispa et al., 2004). In these mice, either *Eda* or its receptor *Edar* is overexpressed under keratin 14 promoter which drives transgene expression as early as E9.5 in the ectoderm and later it becomes restricted to basal layer of the skin and its ectodermal organs (Byrne et al., 1994). *K14-Eda* mice show enlargement of several ectodermal organs or formation of additional skin accessory structures. These mice have increased sweat production, abnormal hair development, longer nails as well as extra teeth and mammary glands (see also 1.3.3.3.). Similarly, *K14-Edar* mice show altered morphogenesis of many ectodermal organs, including the mammary gland, but thus far, only tooth development has been reported in detail (Pispa et al., 2004). Another transgenic mouse line in which a high copy number of wild type *Edar* locus expressed under control of endogenous regulatory elements (Edar^{Tg951}) was generated (Chang et al., 2009, Mou et al., 2008). These mice were shown to have increased size of Meibomian and sebaceous glands as well as an enlarged epithelial compartment for salivary and mammary glands (Chang et al., 2009). Additionally, a mouse mutant with a single amino acid mutation in *Edar* (V370A), associated with upregulated downstream NF-κB signaling, have increased branch density and decreased size of fat pad tissue indicating the role of Eda in the formation of surrounding mesenchymal tissue (Kamberov et al., 2013).

1.3.3.3. From mammary line to buds

In mice, the earliest epithelial molecular sign of mammogenesis is the expression of Wnt reporter TOP-gal *LacZ* in a punctate fashion along curved bilateral lines connecting the fore and hind limb buds at E10.5 (Fig. 1 and 2) (Chu et al., 2004). This expression was found to also be present in mesenchymal cells marking the prospective place of milk line formation. At approximately E11.25, pseudostratified band positive for *Wnt10b* mRNA appears as an arc line between the fore and hind limbs connecting future placodes 2, 3, and 4. Two additional *Wnt10b* positive lines emerge slightly later in development around the fore and hind limb marking the prospective locations of placodes 1 and 5, respectively (Veltmaat et al., 2004). These lines that eventually connect have been regarded as the long disputed murine milk line (Veltmaat et al., 2003). The expression of *Wnt10b* was shown to localize with a wider band of *Wnt6* expression present in the surface ectoderm. Eventually *Wnt10b* becomes restricted to placodes followed by the expression of *Wnt10a* (Veltmaat et al., 2004). Other Wnt pathway members are also expressed during early mammary gland development: *Wnt3* in the epithelium, *Wnt5a*, and *Wnt11* in the mesenchyme surrounding mammary rudiment (Fig. 5) (Christiansen et al., 1995, Chu et al., 2004).

The milk line forms at the dorso-ventral border on the mouse flank and several signaling pathways are involved in initiation and positioning of the milk line (Fig. 5). *Tbx3*, belonging to the T-box transcription factor family, was shown to be expressed as a thin line in the mesenchyme under the presumptive milk line at approximately E10.25 (Jerome-Majewska et al., 2005). In turn, the extent of ventral *Tbx3* expression has been proposed to be controlled by the inhibitory effect of *Bmp4*, whereas *Tbx3* is essential for later Wnt expression (Fig. 5) (Cho et al., 2006). Around the same time as appearance of *Tbx3* expression, *Fgf10* has been shown to be expressed at the center and tip of the thoracic somites underlying the presumptive position of the milk line (Veltmaat et al., 2006). Deficiency in either *Fgf10* or *Fgfr2b* results in absence of *Lef1* and *Bmp4* expression indicating that it lies upstream of these signaling pathways (Mailleux et al., 2002). In support of *Fgf10's* role in determining the milk line localization is the fact that *Pax3* mutants, in which thoracic somites undergo ventral extension, show dorsalization of the mammary line (Veltmaat et al., 2006). *Fgf10* might be, in turn, regulated by *Gli3* and *Hoxc8*, as it was shown that in $Gli3^{Xt-J/Xt-J}$ mouse mutants *Fgf10* expression is reduced in the somites and *Hoxc8*, when mis-expressed, induced somitic *Fgf10* and ectopic placodes (Carroll and Capecchi, 2015, Veltmaat et al., 2006). However, precise regulation remains to be elucidated. Neuregulin 3 (Nrg3) has been proposed to serve as intervening molecule that relay somitic *Fgf10* through the mesoderm to the ectoderm (Fig. 5) (Howard et al., 2005). *Nrg3* is initially expressed in dermal mesenchyme at E11.0 and it becomes restricted to the mammary epithelial cells by E12.0 (Wansbury et al., 2008). Hypomorphic mutants *Nrg3*^{Ska} show no disruption in *Fgf10* and *Tbx3* expression indicating that they may lie upstream of Nrg3 signaling (Howard et al., 2005).

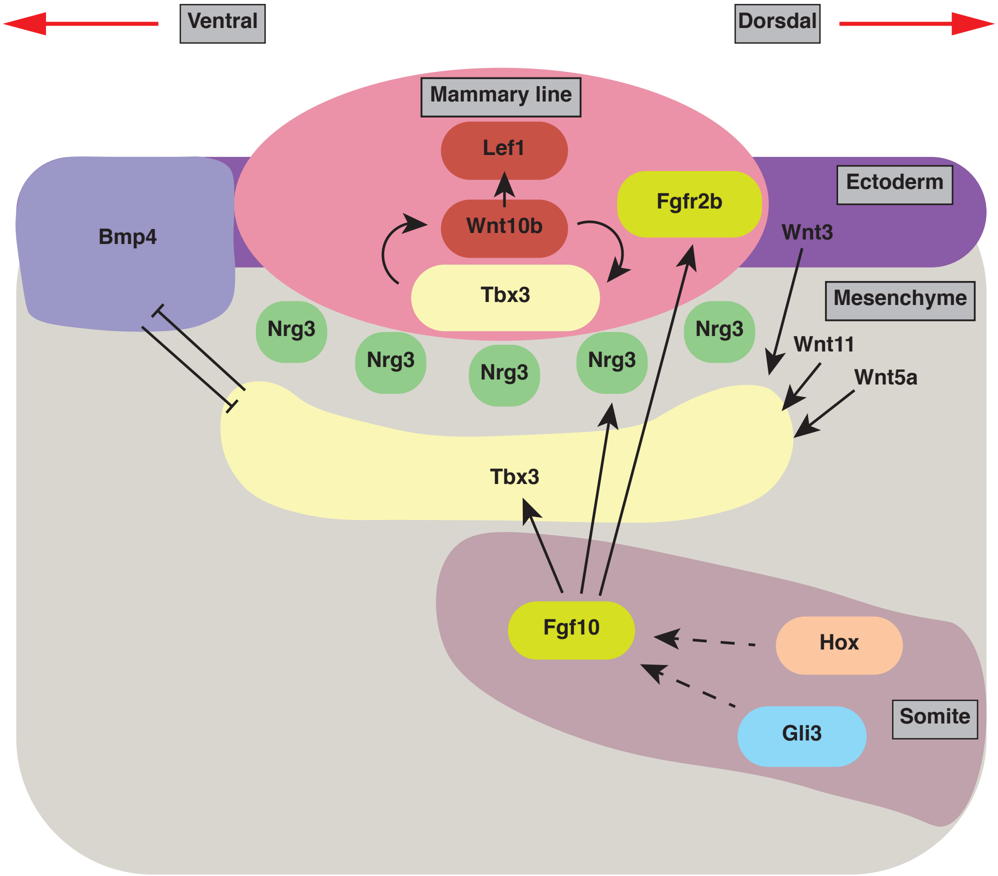

Figure 5. Schematic representation of mammary line specification.
The mammary line is specified by antagonism between dorsal Tbx3 and ventral Bmp4. Fgf10 secreted from cells at the tip of the somite activates Fgfr2b. Tbx3, Wnt10b, and Lef1 become upregulated along the mammary line. For simplicity, the mammary mesenchyme has been omitted in the figure.

The functional importance of many of the molecular regulators of embryonic mammary gland development have been revealed by mouse mutants (see Table 1). Overexpression of Wnt inhibitor *Dkk1* leads to complete inhibition of mammogenesis indicating the crucial role of Wnt in mammary rudiment formation (Andl et al., 2002, Chu et al., 2004). *Lef1* deficient mice have a reduced number of mammary rudiments suggesting that other members of the TCF/Lef family might act redundantly (Van Genderen et al., 1994). Mouse models in which *Pygopus 2* (Wnt modifier), *Lrp5* and *Lrp6* were individually deleted had absent or smaller placodes (Gu et al., 2009, Lindvall et al., 2006, Lindvall et al., 2009). Other signaling pathways that affect mammary placode formation and maintenance include the Fgf signaling pathway. *Fgf10*$^{-/-}$ and *Fgfr2b*$^{-/-}$ mice fail to develop mammary rudiments except for mammary primordium 4 (Mailleux et al., 2002). In addition, the only formed mammary rudiment 4 undergoes apoptosis at E12.5 in *Fgfr2b*$^{-/-}$, however, the development of this primordium proceeds to subsequent stages in *Fgf10*$^{-/-}$. This result indicates that additional Fgfr2b ligand(s) is involved in the maintenance of mammary primordia (Mailleux et al., 2002). Mammary placode fate is promoted by the Eda/NF-κB pathway as supernumerary placodes (a.k.a ectopic placodes) were shown to form between mammary rudiments 3 and 4 in *K14-Eda* mice (Mustonen et al., 2004). Deletion of transcription factor *Tbx3* leads to the failure in mammary placode development with occasional formation of mammary rudiment 2 (Davenport et al., 2003). *Nrg3*^{Ska} mice fail to develop mammary rudiment 3 and ectopic mammary placode forms close to mammary rudiment 4 (Howard et al., 2005). Supernumerary mammary rudiments and nipples developed adjacent to the mammary line in mice overexpressing *Nrg3*. (Panchal et al., 2007).

Table 1. Selected list of mouse mutants with a mammary placode (MP)/bud phenotype.

Mouse model	**Phenotype**	**Reference**
K14-Dkk1	No placode	(Andl et al., 2002)
Lef1$^{-/-}$	MP1, 4, 5 present. Degenerate later	(Van Genderen et al., 1994)
Pygo2$^{-/-}$	Small placodes/buds	(Gu et al., 2009)
Lrp5$^{-/-}$ or *Lrp6*$^{-/-}$	Small placodes/buds	(Lindvall et al., 2006, Lindvall et al., 2009)
Fgf10$^{-/-}$	Only MP4 present	(Mailleux et al., 2002)
Fgfr2b$^{-/-}$	Only MP4 present	(Mailleux et al., 2002)
K14-Eda	Ectopic placodes	(Mustonen et al., 2004, Mustonen et al., 2003)
Tbx3$^{-/-}$	MP2 occasionally present	(Davenport et al., 2003)
Nrg3^{Ska}	Occasionally ectopic MP present close to MP4. MP3 missing	(Howard et al., 2005)
K14-Nrg3	Ectopic placodes	(Panchal et al., 2007)
Msx1$^{-/-}$,*Msx2*$^{-/-}$	Small placodes, do not progress after bud stage	(Satokata et al., 2000)

In summary, *Bmp4* and *Tbx3* define the mammary zone on the dorso-ventral border and are also influenced by *Fgf10*, *Gli3*, and *Hoxc8* whereas *Nrg3* serves as an intervening molecule. Signaling pathways such as Wnt, Eda, Hh, and Egf intersect and reinforce one another in a complex way that remains obscure, to promote critical thresholds of placodal *Tbx3* and Wnts crucial for sustaining mammary fate.

1.3.3.4. From buds to branches

The transition from placode (E11.5) to hillock (E12.5) stage and the ensuing ductal outgrowth with branching morphogenesis is regulated by the interplay between many signaling pathways. *PTHrP* is expressed in mammary epithelial cells from E11.5 onwards whereas *PTHR1* localizes to dense mammary mesenchyme and at E15.0 shows higher expression levels in the upper dermis close to the mammary neck (Fig. 6) (Wysolmerski et al., 1998). Although initiation and early mammary gland development proceeds relatively normally, deletion of either *PTHrP* or *PTHR1* results in failure of mammary rudiment progression beyond bud stage, lack of ductal morphogenesis and nipple development (Wysolmerski et al., 1998, Foley et al., 2001). Subsequent studies have dissected the role of PTHrP as a key regulator governing differentiation of the mammary mesenchyme through activation of Wnt signaling in mesenchyme (Fig. 6) (Dunbar et al., 1999, Foley et al., 2001, Wysolmerski et al., 1998, Hiremath et al., 2012). In turn, specified mammary mesenchyme is capable of responding to Bmp4 signaling, as PTHrP upregulates expression of *Bmpr1a* (Fig. 6) (Hens et al., 2007). Consecutively, *Bmpr1a* leads to activation of transcription factor *Msx2* within mesenchymal cells that enables suppression of hair follicle formation in the overlying nipple skin (Fig. 6). In addition, *Msx2* and the related *Msx1* are expressed in epithelial cells. Although loss of either of these genes has no effect on the mammary rudiment formation, double knock out mice form small placodes that fail to progress after bud stage (Satokata et al., 2000).

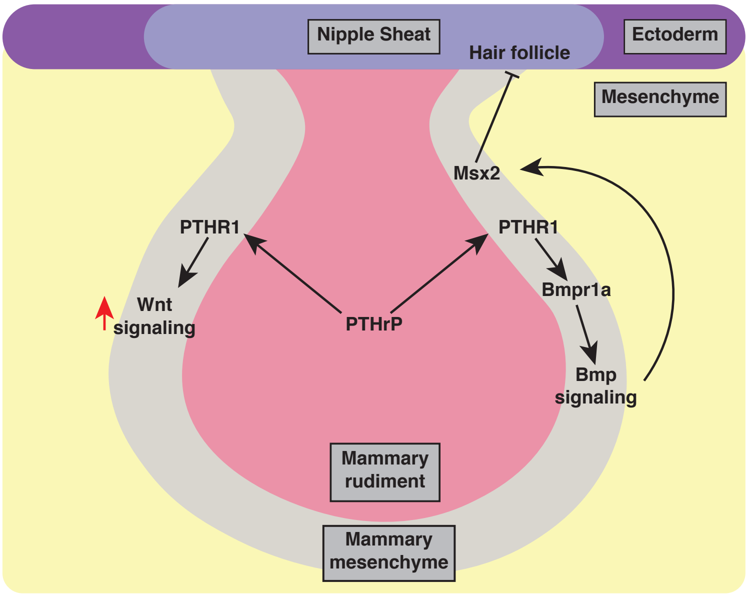

Figure 6. Schematic showing mammary mesenchyme specification *PTHrP expressed in the mammary rudiment actives PTHR1 in the mammary mesenchyme leading to Wnt upregulation. In addition, PTHrP signaling upregulates Bmpr1a which in turn leads to activation of Msx2 and ihibition of hair follicle formation in the nipple sheat.*

For proper mammary rudiment formation, Hh signaling has to be suppressed as evident from the studies showing *Gli3*$^{Xt\text{-}J/Xt\text{-}J}$ mouse mutants' mammary primordia 3 and 5 fail to develop and mammary primordium 2 exhibits defects in rudiment invagination (Lee et al., 2011, Hatsell and Cowin, 2006). Abnormal mammary bud shape and supernumerary nipples were reported in a potent Wnt inhibitor *Sostdc1*$^{-/-}$ knockout mice (Narhi et al., 2012). In these embryos, elevated expression levels of Wnt signaling, marked by *Lef1* and TOP-gal, was shown along the milk line and close to the mammary rudiments in later stages. Similarly, embryos deficient for *Lrp4*, which is the receptor for Sostdc1, exhibit higher levels of Wnt signaling along the milk line, failure in proper bud invagination, and fusion of mammary primordia 2 and 3 (Ahn et al., 2013). Stunted ductal outgrowth of mammary rudiment were reported in Wnt pathway mutants such as *Lrp6*$^{-/-}$ and *Pygo2*$^{-/-}$ (Gu et al., 2009, Lindvall et al., 2009). Additionally, embryos deficient for *Hoxc6*, a member of the Hox family of transcription factors, do not form a branched ductal tree and exhibit smaller mammary fat pads (Garcia-Gasca and Spyropoulos, 2000). Conversely, *Eda* overexpressing mice show precocious branching morphogenesis and increased number of ductal tips, whereas *Eda null* embryos displayed reduced number of branches and ductal length (Voutilainen et al., 2012).

In summary, PTHrP plays a critical role in induction of mammary mesenchyme differentiation, acting through Wnt and Bmp signaling, and as consequence leading to suppression of hair follicle formation in the overlaying nipple skin. Action of signaling pathways such as Eda and Wnt, and Hox family of transcription factors regulate mammary ductal branching.

1.3.4. Cellular mechanisms driving embryonic mammary gland development

Although molecular regulation of embryonic mammary gland development has been described to some extent, cellular mechanisms governing mammogenesis are still poorly understood. The role of cell proliferation in early embryonic stages was first assessed by Boris Balinsky who counted mitotic indexes across E11.0-E14.0 stages based on the appearance of nuclei in histological sections (Balinsky, 1950, Balinsky, 1952). The results showed that the mitotic index in mammary rudiment was significantly lower than in the ectoderm. However, due to technical limitations and to increase statistical power, the data were pooled from all stages concealing discrete changes that might occur between stages (Balinsky, 1950). Balinsky hypothesized that as an alternative for cell proliferation, cell migration might function as a driving force for mammary gland formation (Balinsky, 1952). In rabbit at E13.5 (of note rabbit gestation time is approximately 30-32 days), milk line is morphologically discernible as a ridge elevated above surface ectoderm (Propper, 1978, Wilson and Dudley, 1952). The images from scanning electron microscopy from rabbit embryo revealed cells with filopodia-like extensions along the ridge suggesting that cell migration might be involved in the mammary rudiment formation (Propper, 1978). These data were subsequently extrapolated to the murine milk line. In line with possible cell migration taking place in murine mammary gland formation is the pattern of *Lef1* expression as visualized by in situ hybridization method (Mailleux et al., 2002). Between E11.5 and E11.75 *Lef1* is first expressed in a comet-like shape along the presumptive milk line and becomes restricted to round shape by E11.75. In addition, expression of Wnt pathway markers such as *Wnt10b* or TOP-gal showed similar patterns and positive cells aligning along the milk line indicative of possible cell migration involved (Chu et al., 2004, Veltmaat et al., 2004). Nonetheless, cell migration has been speculated in mammogenesis, yet no experimental evidence exists. Live imaging would be an ideal method to assess this hypothesis, yet mammary gland culturing techniques have been troublesome in this regard.

The notion of low cell proliferation status in mammary rudiments during early developmental stages was subsequently confirmed by tritiated thymidine (^{3}H-TdR) incorporation analysis on histological sections in injected pregnant females (Robinson et al., 1999). Embryos harvested several hours post injection at E13.0 showed no incorporation of ^{3}H-TdR in mammary rudiment whereas embryos collected 24 hours post injection contained ^{3}H-TdR positive cells in the neck of mammary rudiment 3. The facts that ^{3}H-TdR degrades rapidly when not incorporated by cells and lack of positive cells found several hours after injection suggest that observed ^{3}H-TdR positive cells in the mammary rudiment neck might come from adjacent epidermis. Nonetheless, in this study authors neither analyzed this possibility nor tested stages before E12.0 for cell proliferation. A thorough analysis in which the authors assessed all mammary primordia between E11.5 and E13.5 stages was published years later (Lee et al., 2011). In this study, cell proliferation was determined by thymidine analog, 5-bromo-2'-deoxyuridine (BrdU) on histological sections and it was shown that cell proliferation is significantly lower in mammary epithelium as compared to epidermis in all stages analyzed. Similarly to the results observed with ^{3}H-TdR assay, BrdU positive cells were detected in the mammary rudiments' neck after a 24 hours chase. Consequently, cell incorporation was concluded to be the driving force for the initial mammary primordium growth. In addition to this mechanism, cell hypertrophy has been suggested as a complementary driver of growth (Lee et al., 2011). However, this study did not present any quantitative data to support this conclusion. To date only one publication describes the volume of mammary epithelial cells (Kogata et al., 2014). In this study, the authors analyzed cell size in 3D, but only at one developmental stage and as a comparison to *Nrg3*^{ska} mouse mutant.

In summary, the cellular mechanisms driving embryonic mammary gland development have been recognized only to some extent indicating cell migration and cessation of cell cycle as the main mechanisms driving mammogenesis. Cellular processes involved in later developmental stages such as sprouting, invasion to the fat pad and mechanisms of embryonic branching morphogenesis remain to be determined.

1.3.5. Implications of embryonic mammary gland studies in breast cancer

Even though breast cancer influences both sexes, it is the most common cancer affecting women worldwide (Bray et al., 2018). The numbers of women diagnosed with this life changing disease are expected to rise in successive generations due to improved diagnostics and increasing life expectancy. Therefore, it is critical to have a better understanding of breast cancer and translate this knowledge to possible treatment options. Lack of access to human tissue led to use of the mouse as a model organism for deciphering mechanisms underlying breast cancer predominantly in postnatal stages. The significance of these studies is immense, however, the relevant information for breast cancer knowledge might still come from the research on embryonic mammary gland development.

Many signaling pathways that are involved in embryonic mammogenesis such as Wnt, Hh, Fgf, Egf, and PTHrP have been implicated in the breast cancer metastasis and maintenance of breast cancer stem cells (Butti et al., 2019, Howard and Ashworth, 2006). As an example, members of the Wnt pathway, *Wnt3a*, *Wnt6*, and *Wnt10b*, are involved in mammary specification and early morphogenesis. They have been shown to be genetically altered in MMTV-induced mammary tumors as well as overexpressed in many breast cancer cell lines (Benhaj et al., 2006, Callahan, 1996). Therefore, expanding our knowledge on the regulation of these signaling pathways and their coordination for proper morphogenesis may help to understand how they are modulated in pathological conditions such as cancer.

Epithelial-mesenchymal interactions are vital for supporting both prenatal and postnatal mammary gland development. Growing evidence suggests that abnormal stroma with deregulated extracellular matrix facilitates the formation of the tumor microenvironment and consequently promotes breast cancer (Howard and Lu, 2014). Tissue recombination studies show that embryonic mammary mesenchyme is capable of supporting growth of murine mammary tumor cells resulting in the formation of a mammary duct (Decosse et al., 1973). This raises the question of the similarity between embryonic mammary mesenchyme and breast cancer stroma. Promising results are coming from studies improving therapy outcome by normalizing breast cancer tumor microenvironment (Chauhan et al., 2019, Panagi et al., 2020). This indicates the importance of understanding normal tissue stroma in battling breast cancer.

In summary, many mechanisms, either molecular or cellular, observed in normal mammary gland development are recurring in breast cancer such as cell proliferation, cell migration, and cell invasion to the fat pad. Better understanding of these processes in a native environment may translate into greater knowledge of breast cancer and possible therapy options for patients.

2. AIMS OF THE STUDY

Prior to the work presented in this thesis, the Eda/NF-κB pathway had been shown to promote placodal cell fate and formation of ectopic mammary placodes (Mustonen et al., 2004, Mustonen et al., 2003). Additionally, in later developmental stages the Eda/NF-κB pathway had been reported to induce precocious branching morphogenesis (Voutilainen et al., 2012). However, the exact mechanism of how Eda stimulated cell fate in placode formation and Eda target genes in mammary rudiment were unknown. Moreover, cellular mechanisms regulating early mammary primordium formation were poorly defined.

Aims of the thesis were:

1. To identify novel Eda/NF-κB regulated genes involved in mammary cell fate specification and placode morphogenesis
2. To decipher the cellular mechanisms involved in early embryonic mammary gland formation and mammary gland invagination into underlying mesenchyme

3. MATERIAL AND METHODS

In this thesis work mouse was used as a model organism to answer the questions of molecular and cellular mechanisms driving early mammary gland development. Genetically modified mice were made and maintained in *NMRI*, *C57BL/6*, *FVB*, and *Hsd:ICR(CD-1)* backgrounds as described in the original articles. All mouse experiments were approved and carried out in accordance with the guidelines of the Finnish national animal experimentation board.

Table 2. List of mouse models used in this thesis.

Mouse strain	**Description**	**Reference**	**Used in publication**
NMRI	Wild type outbred strain	Envigo	I
C57BL/6	Wild type inbred strain	Charles River	I
TOP-gal	Wnt pathway reporter	(Dasgupta and Fuchs, 1999)	I, III
NF-κB gal	NF-κB pathway reporter	(Bhakar et al., 2002)	I, III
K14-Eda	Eda overexpression model	(Mustonen et al., 2003)	I, II
Eda$^{-/-}$ *(Tabby)*	Eda null model	Jackson Laboratories (Stock 000338)	I, II
IκBαΔN	NF-κB suppressed model	(Schmidt-Ullrich et al., 2001)	I
Fgf20$^{LacZ/LacZ}$	Fgf20 null model	(Huh et al., 2012)	II, III
R26R^{tdTomato}	Ubiquitous fluorescent reporter	Jackson Laboratories (Stock 007914)	III
R26R^{CreERT2}	Ubiquitous inducible Cre recombinase model	Jackson Laboratories (Stock 008463)	III
R26R$^{mT/mG}$	Ubiquitous fluorescent reporter	Jackson Laboratories (Stock 007576)	III
TCF/Lef1:H2B-GFP	Wnt pathway reporter	Jackson Laboratories (Stock 013752)	III
Myh9 floxed	*Myh9* gene floxed model	(Leon et al., 2007)	III
K14-Cre	Constitutive Cre recombinase model active in epidermis	(Hafner et al., 2004)	III
K14-Cre43	Constitutive Cre recombinase model active in epidermis	(Andl et al., 2004)	III
Fucci	Fluorescent ubiquitous cell cycle indicator model	(Sakaue-Sawano et al., 2008)	III
R26R-RG	Ubiquitous fluorescent reporter	(Shioi et al., 2011)	III
K17-GFP	Fluorescent reporter of epithelial appendages in embryonic development	(Bianchi et al., 2005)	III

Methods and techniques used in this thesis are described in detail in the original publications.

Table 3. List of the methods and techniques used in this thesis.

Method	**Used in publication**
Immunological detection of protein	
Immunohistochemistry	I, II
Immunofluorescence	I, II, III
Gene expression analysis	
Whole-mount RNA *in situ* hybridization	I, II
Non-radioactive RNA *in situ* hybridization on tissue sections	I
Radioactive RNA *in situ* hybridization on tissue sections	I
Quantitative RT-PCR	I, II
Affymetrix Mouse Exon 1.0 ST microarray	I
Microscopy	
Bright field microscopy	I, II
Fluorescent microscopy	I, II
Confocal microscopy	II, III
Scanning electron microscopy	I, III
(Spinning disk) confocal live imaging	III
Tissue culture	
Mammary placode formation	I
Others	
Histology	I, II
Carmine alum staining of mammary glands	I, II
X-gal staining	I, II
Cell proliferation assay (EdU)	III

Following primary antibodies were used for immunostaining data in listed publications.

Table 4. List of primary antibodies used in this thesis.

Antibody	**Manufacturer**	**Used in publication**
Keratin2e	Fitzgerald	I
Madcam1	BD Pharmingen	I
β-Galactosidase	MP Biomedicals	II, III
Ki-67	Abcam	II
Caspase-3	Cell Signaling Technology	II
Keratin 8	DSHB	II
Keratin 14	Neomarkers	II
ERα	Dako	II
PR	Thermo Scientific	II
αSMA	Abcam	II
Lef1	Cell Signaling Technology	II, III
p63	Neomarkers	II
EpCAM	BD Pharmingen	III
GM130	Sigma-Aldrich	III
pMLC	Cell Signaling Technology	III
NMIIA	BioLegend	III

For analysis of gene expression pattern by radioactive and non-radioactive RNA *in situ* hybridization ^{35}S-UTP labelled and digoxigenin labelled probes were used, respectively. The following table summarizes probes that were utilized and their original references.

Table 5. List of the probes used in this thesis.

Probe	**Reference**	**Used in publication**
Lgr4	article I	I
Kremen2	article I	I
Dkk4	(Fliniaux et al., 2008)	I, II
Lef1	(Travis et al., 1991)	I, II
Wnt10a	(Dassule and Mcmahon, 1998)	I
Wnt10b	(Wang and Shackleford, 1996)	I, II
β-cat	(Laurikkala et al., 2002)	I, II
Shh	(Vaahtokari et al., 1996)	I
PTHrP	(Voutilainen et al., 2012)	I, II
Nrg3	(Howard et al., 2005)	I
Tbx3	(Howard et al., 2005)	I
Mmp9	article I	I
Adamts15	article I	I
Edar	(Laurikkala et al., 2001)	I, II
Eda	(Laurikkala et al., 2001)	I
Fgf20	article II	II

4. RESULTS AND DISCUSSION

4.1. DOWNSTREAM TARGET GENES OF EDA/NF-κB IN MAMMARY RUDIMENTS (I, II)

The Eda/NF-κ B signaling pathway is known to promote placodal cell fate, as overexpression of *Eda* under keratin 14 promoter leads to ectopic formation of several ectodermal accessory structures including mammary gland (Mustonen et al., 2004, Mustonen et al., 2003). Of note, keratin 14 is expressed already at E9.5, first seen in the ectoderm overlying somites and by E13.5 occurred in most lateral areas of the embryo (Byrne et al., 1994). Therefore, it was of interest to identify the downstream target genes of this signaling pathway to gain better understanding how mammary cell fate is regulated.

To determine the immediate downstream target genes of Eda/NF-κB, E13.5 mammary buds from *Eda*$^{-/-}$ mice were exposed to recombinant Fc-Eda protein or control medium for four hours and a microarray of expressed genes was performed on extracted RNA samples. Upon Eda treatment, 245 genes were significantly upregulated whereas 78 genes were downregulated (Publication I, S1 Table). We found signaling pathways such as Wnt, Fgf, TNF, Tgfß, chemokine and Hh to be regulated by Eda treatment (see Table 6). Additionally, among upregulated genes we identified chloride channel proteins *clca1* and *clca2*, adhesion molecules *Madcam1* and *Icam1*, transcription factor *Foxi3*, extracellular matrix degrading metalloproteinases *Adamts15* and *Mmp9*, and members of Fgf family *Fgf17* and *Fgf20* (see Table 6). Our group has previously profiled Eda/NF-κ B downstream targets in hair follicle showing significant changes in expression of Wnt, Fgf, TNF, and chemokine pathway genes, similarly to mammary rudiment (Lefebvre et al., 2012). Although these studies used different microarray platforms and comparison needs to be done consciously, the tendency of Eda to regulate the analogous gene regulatory network between hair follicles and mammary rudiments is apparent, with no striking differences.

In order to validate the results obtained from the microarray, we performed quantitative real-time reverse-transcriptase-PCR (qRT-PCR) on E13.5 *Eda*$^{-/-}$ mammary buds exposed to short Fc-Eda treatment for four hours and in situ hybridization (ISH) of selected genes: *clca1/2*, *Adamts15*, *Mmp9*, *Icam1*, *Madcam1*, *Kremen2*, *Lgr4*, *Fgf17*, and *Fgf20*. Among 9 tested genes all showed the same tendency as in the microarray, however, when assessed by qRT-PCR only 7 were statistically significantly upregulated by short Fc-Eda treatment: *Adamts15*, *Mmp9*, *Icam1*, *Kremen2*, *Lgr4*, and *Fgf20* (Publication I, Fig. 6, Publication II, Fig. 1A). Of note, analysis of the absolute mRNA quantity revealed that *Fgf17* is expressed at a very low level, therefore, it was not analyzed further. Using ISH or X-gal staining, we confirmed the upregulated expression of *Madcam1*, *Kremen2*, *Lgr4*, *Mmp9*, and *Fgf20* in *K14-Eda* embryos, however, we did not detect *Icam1* or *Adamts15* transcripts in developing mammary primordia (Publication I, Fig. 7 and Fig. S2, Publication II, Fig. 2). These results show that several of the genes we have tested lie downstream of Eda in mammary buds. Interestingly, *Lgr4*, a regulator of mammary gland development and stem cell activity,

Table 6. List of selected genes upregulated upon Eda treatment. Log2 indicates (log2(Fc-Eda-treatment)-log2(control)).

	Gene	**log2**
Wnt pathway	*Dkk4*	2.00
	Wnt10b	1.13
	Wnt10a	0.94
	Lrp4	0.93
	Kremen2	0.81
	Lef1	0.46
	Lgr4	0.35
Fgf pathway	*Fgf17*	0.97
	Dusp6	0.83
	Fgf20	0.35
Other genes	*Clca2*	2.3
	Clca1	1.8
	Madcam1	1.7
	Foxi3	1.43
	Adamts15	1.13
	Mmp9	1.06

was shown to be expressed in embryonic mammary progenitor cell lines (Kogata et al., 2018, Wang et al., 2013). It would be interesting to elucidate if Eda plays a role in stem cell maintenance in mammary rudiment. Among the upregulated genes by Eda, we found many belonging to Wnt pathway including both agonists (*Wnt10a*, *Wnt10b*, *Lef1*, and *Lgr4*) and antagonists (*Lrp4*, *Kremen2*, and *Dkk4*) (see Table 6). Similar observations have been made for hair follicle (Fliniaux et al., 2008, Voutilainen et al., 2012, Zhang et al., 2009). It appears that Eda fine tunes several pathways, involved in proper spacing of ectodermal accessory structures through the reaction-diffusion model, by modulating activators and inhibitors of placode formation (Kondo and Miura, 2010, Painter et al., 2012). This would serve as a possible explanation for the puzzling phenotype observed in HED patients which may have both missing and supernumerary nipples (Clarke et al., 1987, Megarbane et al., 2008).

4.2. EDA/NF-κB TARGET GENE FGF20 REGULATES MAMMARY BUD SIZE (II)

Fgf20 is a member of the Fgf9 subfamily comprised of Fgf9, Fgf16, and Fgf20, and it has been shown to be an important downstream effector of Eda in developing hair follicles and teeth (Haara et al., 2012, Huh et al., 2013, Lefebvre et al., 2012). Therefore, we decided to explore the role of Fgf20 in mammogenesis. Taking advantage of the *Fgf20-LacZ* knock-in allele, we performed X-gal staining on *Fgf20*$^{LacZ/+}$ embryos throughout embryonic mammary gland development (Publication II, Fig. 1B, C, E-H) (Huh et al., 2012). The earliest detectable expression we observed was at around E11.25 in the mammary rudiment 1 and by E11.5 it was confined to mammary rudiments 1 and 3. By E13.5, all mammary rudiments showed the expression of *Fgf20*. The *Fgf20-LacZ* signal remained relatively strong in mammary primordia until E15.5 but it was substantially downregulated at E16.5. From E18.5 onwards no expression of *Fgf20* was detected in the mammary gland in postnatal stages (Publication II, Fig. 1H and Fig. S1B-H).

To study the influence of Eda on *Fgf20* expression levels *in vivo* we utilized *Eda null*, *Eda overexpression*, and *Fgf20*$^{LacZ/+}$ models (Publication II, Fig. 2). The onset of *Fgf20-LacZ* expression was delayed in *Eda*$^{-/-}$ embryos at E11.5 and the signal was somewhat decreased at E12.5 as compared to control or *K14-Eda* embryos. At E13.5-E14.5 in *K14-Eda* embryos, the expression appeared more intense than in the rest of the samples, at E15.5 the expression was decreased in *Eda null* whereas in *K14-Eda* it was more profound, thus, correlating with the Eda status. These results showed Eda's influence on *Fgf20-LacZ* expression was rather modest suggesting that some cues other than Eda regulate *Fgf20* expression in mammogenesis. In mice, the *Fgf20* promoter was shown to be highly responsive to β-catenin/Lef1 as tested by promoter-reporter assays, therefore, it is likely that Wnt is a positive regulator (Huh et al., 2013).

To unravel the role of Fgf20 in mammary rudiment formation we analyzed the expression of *Wnt10b* by ISH in *Fgf20 null* (*Fgf20*$^{LacZ/LacZ}$) embryos in early developmental stages (Publication II, Fig. 3A-B). At E11.5, the expression pattern was indistinguishable between knockout and control embryos indicating that loss of *Fgf20* does not affect mammary placode induction and formation. However, at E12.5 *Wnt10b* was expressed at reduced levels in *Fgf20*$^{LacZ/LacZ}$ embryos. This finding was further supported by the quantification of the expression area showing a significant decrease between control and knock out embryos (Publication II, Fig. 3B'). The observed expression reduction prompted us to assess morphology of the mammary buds with the aid of 3D confocal microscopy. The analysis showed that *Fgf20*$^{LacZ/LacZ}$ mammary rudiments were significantly smaller than their control littermates at E13.5 and E15.5 indicating bud size defects (Publication II, Fig. 3C-D'). Our attempt to elucidate the possible molecular regulation behind bud phenotype by ISH at E12.5 showed no gross difference in the expression of *Edar* and *Lef1* (Publication II, Fig. S2). However, *Dkk4* expression pattern was somewhat reduced. These puzzling results, of Fgf20 being not essential for placode induction, yet leading to smaller buds and lower expression of *Dkk4*, might be due to redundancy with other Fgfs, such as Fgf9 which is a member of the same Fgf subfamily. Fgf9 has been shown to be expressed in embryonic mammary glands and redundancy between these two Fgfs has already been demonstrated in developing organs (Barak et al., 2012, Eblaghie et al., 2004, Haara et al., 2012, Huh et al., 2015). In addition, the Fgf9 subfamily is capable of signaling through several Fgfrs, and together with the known differential ligand binding capacities of Fgfs there are dozens of possibilities for context dependent outcomes which could also explain the observed smaller placodes in *Fgf20*$^{LacZ/LacZ}$ model (Ornitz and Itoh, 2015).

Fgf20 signals mainly through the mesenchymally expressed Fgfrs (Zhang et al., 2006), but whether the effects of Fgf20 on mammary gland epithelium are direct, mediated by mesenchymal compartment, or both is currently unknown (Fig. 7). Similar to mammary rudiment, Fgf20 in hair follicle has been shown to be dispensable for placode formation, but it plays a crucial role for condensation of underlying mammary mesenchymal cells required for further follicular downgrowth (Huh et al., 2013). It would be interesting to know the target genes regulated by Fgf20 in mammary rudiment and whether Fgfs play a similar role in the condensation of the primary mammary mesenchyme as in hair follicles.

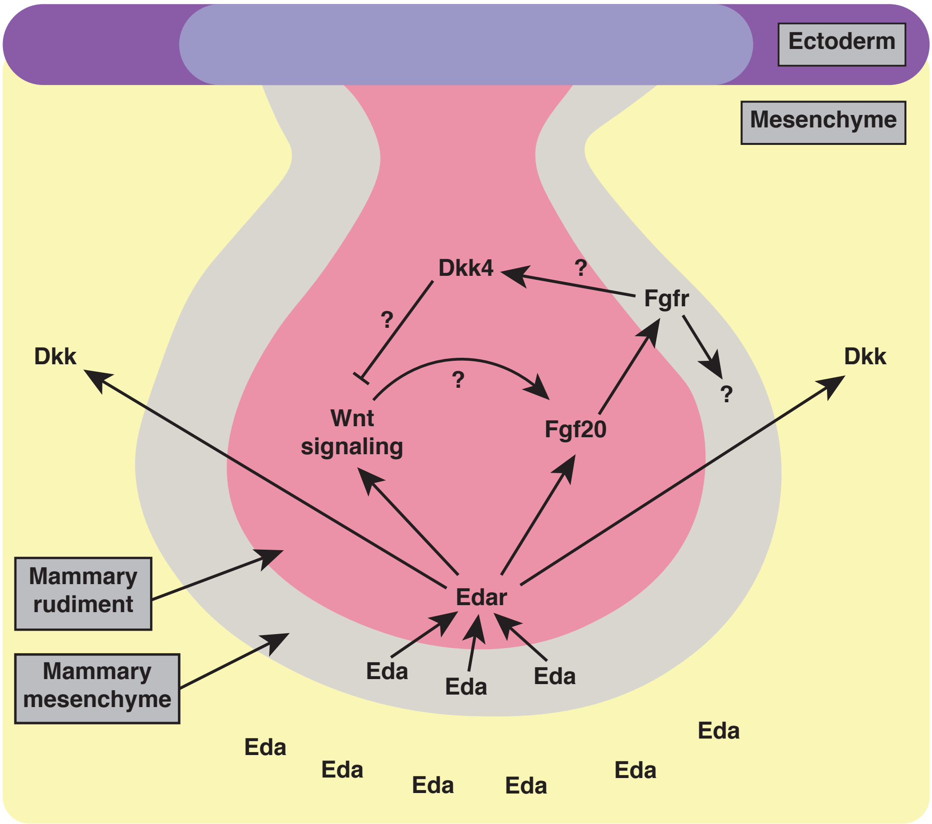

Figure 7. ***Schematic of putative Fgf20, Eda and Wnt pathways interplay.***
Expressed in the mesenchyme, Eda, signals to its receptor Edar in the mammary rudiment. Activation of Eda/NF-κB pathway leads to upregulation of Wnt pathway genes, both agonists and antagonists as evident from microarray data. It is likely that Eda mediates long-range inhibitors (such as Dkk) in the mesenchyme and short-range activators (Wnt pathway in the mammary rudiment), therefore, aiding in proper spacing of ectodermal organs. Activated by Eda/NF-κB pathway Fgf20 signals to its mesenchymal receptor, likely leading to activation of Dkk4 in the mammary rudiment. In turn, Dkk4 acts as inhibitor on Wnt pathway, whereas Wnt signaling is likely a positive regulator of Fgf20. It remains unknown what signals are activated by Fgf20 in mesenchyme.

4.3. FORMATION OF EDA/NF-κB INDUCED ECTOPIC MAMMARY PLACODES IS WNT DEPENDENT (I)

The Eda/NF-κB signaling pathway has been previously shown to induce ectopic mammary rudiments between primordia 3 and 4 (Mustonen et al., 2004, Mustonen et al., 2003). In our study we also found supernumerary primordia forming in the neck region upon Eda overexpression in *K14-Eda* model (Publication I, Fig. 1). The expression of *Wnt10b* and *Dkk4* was confined to forming mammary rudiments 3 and 4 at E11.25 as assessed by ISH in *K14-Eda* and control embryos (Publication I, Fig. 1G-H). To our surprise, these markers showed localized expression in the neck region in both *K14-Eda* and control embryos. We observed similar results with the *NF-κB LacZ* reporter model, yet in *K14-Eda* embryos the expression looked more intense and was confined to up to four small foci (Publication I, Fig. 1A-F) (Schmidt-Ullrich et al., 2001). These results indicate that the region capable of supporting mammary induction, traditionally thought to be located in the area between axilla and the genital tubercle, is longer than previously appreciated (Propper et al., 2013). In line with this result, a previous study describes an additional streak of *Wnt10b* positive cells located dorsally to the milk line that encircles the forelimb on the dorsal side ending at the anterior edge of the forelimb bud (Veltmaat et al., 2004). We found that this is exactly the same location where ectopic placodes in the neck of *K14-Eda* embryos form. After thorough review of the published articles, we found that this region is positive for several placode markers including *Wnt6*, *Tbx3*, and *s-SHIP-GFP* (Jerome-Majewska et al., 2005, Rohrschneider et al., 2005, Veltmaat et al., 2004). Together with our finding these indicate that murine milk line expands past the axillary area.

The ectopic mammary glands in K14-Eda were reported to give rise to nipples with associated ductal system that were responsive to pregnancy hormones (Mustonen et al., 2003). We found that in the *K14-Eda* model supernumerary mammary rudiments in the neck were associated with accessory nipple-like structures (Publication I, Fig. 3A-B). However, when assessed these nipple-like structures did not express keratin 2e, a known specific marker of nipple epithelium indicating that the nipple epithelium was not correctly differentiated (Mahler et al., 2004). Despite these observations, we found that the neck region was able to support ductal morphogenesis and pregnancy-associated morphological changes, yet giving rise to smaller ductal trees than in endogenous glands (Publication I, Fig. 3C-E).

To investigate the formation of ectopic mammary rudiments in more detail, we manipulated mammary placode formation *ex vivo* (Voutilainen et al., 2013). Explants isolated from *K14-Eda* and control littermate embryos at E12.5 were cultured for two days (Publication I, Fig. 8A-C). After one day of culture (E12.5 + 1d), wild type and *K14-Eda* samples showed no obvious difference as assessed by stereomicroscope. Visible changes appeared by E12.5 + 2d, as in *K14-Eda* explants supernumerary bud-like structures formed between mammary buds 3 and 4, and occasionally between buds 2 and 3. We found that usually 2-3 supernumerary primordia appeared between mammary buds 3 and 4, therefore, explants recapitulated the *in vivo* phenotype closely (Mustonen et al., 2004).

Given that our microarray and qRT-PCR analyses identified several Wnt pathway genes upregulated upon Eda treatment and these genes (*Wnt10a*, *Wnt10b*, *Kremen2*, *Lgr4*, *ß-cat*) showed streak-like expression patterns between buds 3 and 4 in *K14-Eda* embryos at E12.5 as assessed by ISH, we turned to determine the effect of Wnt pathway on *K14-Eda* samples in cultured explants (Publication I, Fig. 7A-E). We cultured E12.5 wild type and *K14-Eda* explants in the presence of canonical Wnt pathway inhibitor, XAV939, and confirmed that exposure to XAV939 led to significant downregulation of Wnt pathway activity as seen in all TOP-gal samples (17/17 explants) (Publication I, Fig. 9) (Huang et al., 2009). Supernumerary placodes were always detected in control *K14-Eda* samples at E12.5 + 2d, however, we observed a significant reduction in their number by low dose (10 µM) and near to complete absence by high dose (40 µM) of XAV939. Of note, XAV939 had no apparent effect on endogenous rudiments at these concentrations in either wild type or *K14-Eda* samples. We exposed explants expressing K17-GFP, a marker of forming mammary primordia, to XAV939 at the time when placodes first appear (E11.0) (Publication I, Fig. S5) (Bianchi et al., 2005). Concentration of 40 µM did not prevent emergence of mammary placodes, yet their size was clearly reduced. It suggests that supernumerary mammary placodes are more sensitive to the reduction of Wnt signaling than endogenous ones. This could be explained by the fact that Wnt pathway, crucial for mammogenesis (*K14-Dkk1* mice lack mammary rudiments) is already present at E10.5 as shown by Wnt10b and TOP-gal expression (Andl et al., 2002, Chu et al., 2004, Veltmaat et al., 2004). Therefore, mammary cell fate specification occurred before the XAV939 treatment leading to smaller but not absent mammary placodes. These data indicate that Eda signaling upregulates Wnt activity within the mammary line which results in ectopic mammary placode formation. These two signaling pathway are known to interplay during development of several ectodermal organs (Arte et al., 2013, Cui et al., 2014, Fliniaux et al., 2008, Voutilainen et al., 2013, Zhang et al., 2009).

In summary, we showed that overexpression of Eda in the *K14-Eda* model leads to ectopic mammary placode formation in the neck region suggesting that murine milk line extends past the axillary area. Additionally, our results indicate that Eda signaling upregulates Wnt activity within the mammary milk line leading to the formation of supernumerary mammary placodes.

4.4. ECTODERMAL CELL HYPERTROPHY AND CELL PROLIFERATION HAVE MINOR CONTRIBUTION IN EARLY MAMMARY RUDIMENT DEVELOPMENT (III)

The cellular mechanisms driving mammary placode formation have remained poorly defined. In this research we used both 3D and 4D confocal microscopy and a number of mouse models to answer open questions regarding embryonic mammary rudiment formation. First, we showed that mammary primordium steadily grows between placode and bulb stages totaling a 2.5-fold increase as assessed by volume analysis from the 3D surface rendering (Publication III, Fig. 1D). This growth was accompanied by changes in the organ shape, from a relatively flat and elongated comet-like form at placode stage to enlarged and rounded sphere with prominent neck at bulb stage (Publication III, Fig. 1A-C). This was confirmed by the analysis of sphericity showing a significant increase between placode and hillock stages (Publication III, Fig. 1E). To date this is the first quantitative descriptive characterization of the mammary rudiment in early developmental stages in 3D.

But what drives growth of the mammary primordium? We analyzed cell size and shape using stochastic and sparse cell labeling. Cytoplasmic expression of the reporter allowed 3D surface rendering of the mammary epithelial and control of epidermal cells. Cell size quantification showed that the mammary epithelial cells were smaller than epidermal cells at placode and hillock stages, whereas there was no significant difference between these cells at bulb stage (Publication III, Fig. 2D). Additionally, the volume of the mammary epithelial cells increased by 1.2-fold between placode and hillock stages, however, further increase was not observed. This volume gain of the mammary epithelial cells suggests that cell hypertrophy contributes to the early mammary rudiment growth, but only modestly. Cell hypertrophy has been previously suggested in mammogenesis (Lee et al., 2011). However, in that study authors concluded that cell hypertrophy contributes between hillock and bulb stages, yet this statement was not supported by any quantitative data.

To date only one study has assessed cell size of the mammary bud with the aid of 3D volume rendering (Kogata et al., 2014). In this work authors analyzed bud and mammary epithelial cell size in control and *Nrg3*^{Ska} mutants showing that *Nrg3*^{Ska} mutants had significantly smaller buds and mammary epithelial cells than controls. These results implicate the Nrg3/Erbb4 pathway as a potential regulator of mammary epithelial cell volume. On the contrary to the observed increase in the cell volume during early mammogenesis, in hair follicle, cell volume was reported to decrease during placode formation suggesting different regulation of cell size in these two ectodermal organs (Ahtiainen et al., 2014).

Since increase in cell size had only a minor contribution to early mammary rudiment growth, we decided to analyze cell proliferation. We used the *Fucci* mouse model in which cells in G1/G0 express nuclear monomeric Kuzabi Orange (mKO2) and cells in S/G2/M express nuclear monomeric Azami Green (mAG1) (Sakaue-Sawano et al., 2008). The quantification showed that the mammary epithelial cells had lower proliferation status as compared to epidermal cells: the mammary rudiments consisted mainly of G1/G0 cells, whereas cells in S/G2/M phases were rare accounting for between 5-9%, a finding confirmed by EdU incorporation assay (Publication III, Fig. 2G and S2C). These observations were consistent throughout the stages analyzed. As shown by these results, cell hypertrophy and cell proliferation have minor contributions to early mammary rudiment growth.

Similarly to mammary primordium, low levels of cell proliferation has been observed at the placode stage in other ectodermal organs such as hair follicle and teeth (Ahtiainen et al., 2014, Ahtiainen et al., 2016). However, after the placode stage, proliferation is resumed and has been shown to be a major driver of growth of these organs (Ahtiainen et al., 2014, Ahtiainen et al., 2016, Ouspenskaia et al., 2016). In this context, mammary rudiment with its prolonged quiescence seems to be unique among other ectodermal organs. Large-scale morphogenetic changes have been linked with downregulation of cell divisions (Schock and Perrimon, 2002). In hair follicle, downregulation of cell proliferation was suggested to be required for cell fate acquisition (Ahtiainen et al., 2014). It is interesting to speculate that prolonged quiescence of cell proliferation might be required for acquisition of mammary cell fate.

4.5. CELL MIGRATION FUELS CELL INFLUX THAT DRIVES EARLY MAMMARY RUDIMENT FORMATION (III)

The modest increase in cell size and the majority of cells being in G1/G0 phases suggested involvement of additional cellular mechanisms in mammary rudiment formation. Cell influx has been proposed to contribute in early mammogenesis (Lee et al., 2011), therefore, we have analyzed total cell number in mammary rudiments between placode and bulb stages. The quantification showed significant increase of total cell number between placode and hillock stages, and subsequent, although not statistically significant, increases between hillock and bulb stages (Publication III, Fig. 2E). The observed increase was 1.6-fold between E11.5 and E13.5 suggesting that a rise in cell number has a major contribution in early mammary rudiment growth.

3D renderings of mammary epithelial cells revealed elongated cells with long protrusions at placode stage, suggesting that these cells could be migratory likely from adjacent epidermis (Publication III, Fig. 2B). Thus, we decided to first analyze the shape of cell nuclei as it is well recognized that cells adapt their shape according to the environment they are in, therefore, cell migration in epithelial tissues would lead to deformation of the biggest organelles such as nuclei (Friedl et al., 2011). Quantification showed that sphericity is significantly lower in mammary epithelial cells than epidermal cells indicating that the mammary epithelial cells are under strain (Publication III, Fig. 3B). This result prompted us to investigate if the mammary epithelial cells exhibit specific polarity at the placode stage that could indicate cell migration and we quantified mammary epithelial cell angle in respect to the placode (Publication III, Fig. 3C-E). It was considered that cells migrating towards the placode would have an angle of less than 90 degrees and cells migrating away would have an angle greater than 90 degrees. The quantification showed that the majority of the mammary epidermal cells had angles less than 90 degrees on the contrary to epidermal cells (Publication III, Fig. 3F). These results obtained from fixed samples were indicative of the possible involvement of cell migration in mammary rudiment formation.

To delineate whether cell migration is in fact driving placode formation, we used previously established whole embryo confocal live imaging (Miroshnikova et al., 2018) and optimized it for E11.25 embryos (Fig. 8, Publication III, Fig. 3G). This allowed us to track epithelial cells up to 6 hours. The analysis revealed that mammary epithelial cells had significantly longer track length and net displacement than epidermal cells (Publication III, Fig. 3H). The quantification of cell tracks showed that the mammary epithelial cells were migrating towards the center of the placode whereas epidermal cells were characterized by random movement (Publication III, Fig. 3I). This is the first time that this phenomenon has been documented by live imaging, 70 years after Boris Balinksy postulated that cell migration is involved in mammary rudiment formation. The advantage of this live imaging method is that it enables imaging of only one area rather than the entire embryo. In this sense the region of interest does not need to be removed from its microenvironment and stress exerted upon dissection is not present. However, the fact that an entire embryo is being imaged means that the imaging window is rather short with a maximum duration of 6 hours for E11.25 embryos. It would be interesting to follow cells behavior for up to 24 hours, yet it is not currently possible with this set-up. In addition, tissue manipulation with beads loaded with soluble molecules is also unsuitable in this method as the embryo is fully submerged into medium.

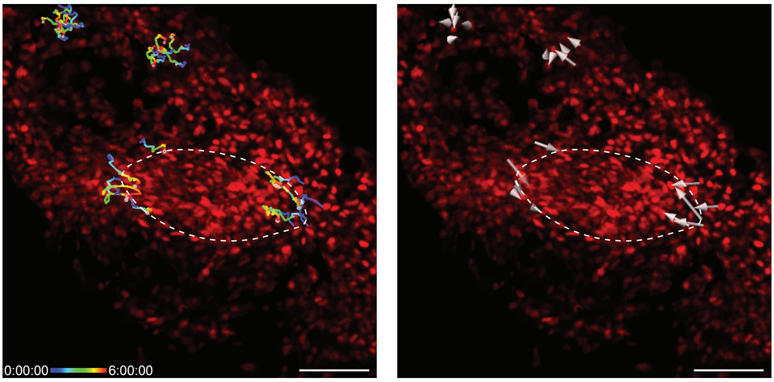

Figure 8. Live imaging of mammary placode at E11.25.
Confocal time-laps 3D imaging. On the left image showing tracks of individual mammary epithelial and epidermal cells expressing Fucci, mKO transgene (nuclear red). On the right vectors of these cells. Dashed line indicates mammary placode. Scale bar, 80 µm.

Similarly to mammary rudiment, the involvement of migration-driven cell influx in ectodermal organ formation has been shown for hair follicle and teeth (Ahtiainen et al., 2014, Ahtiainen et al., 2016). Studies on hair follicle reported that signaling pathways such as Wnt and Eda increased cell motility during hair follicle morphogenesis (Ahtiainen et al., 2014). It is possible that these pathways stimulate mammary epithelial cells in a similar manner. In line with this idea is the fact that upon Wnt inhibition mammary placodes were smaller. However, future studies are required to confirm this possibility.

4.6. EDA/NF-κB PATHWAY HAS MINOR INFLUENCE ON CELL PROLIFERATION DURING MAMMARY RUDIMENT FORMATION (UNPUBLISHED)

The role of Eda/NF-κB signaling in ectodermal appendages development is largely established (Kowalczyk-Quintas and Schneider, 2014). However, the contribution of this pathway to cellular behaviors in the context of mammary rudiment formation remains unexplored.

To answer this question, preliminary data from the *K14-Eda* mouse model was collected and size and shape of the mammary primordium from placode to bulb stages analyzed. 3D quantification showed that the volume did not differ between *K14-Eda* embryos and their control littermates at the placode stage (E11.5) (Fig. 9). Significant volume increase took place at the hillock stage (E12.5) and further increase was detected at the bulb stage (E13.5) in *K14-Eda* embryos as compared to their control littermates, although the shape (sphericity) was unaffected at placode and hillock stages (Fig. 9). However, at bulb stage, control littermate embryos showed significantly higher sphericity than *K14-Eda*.

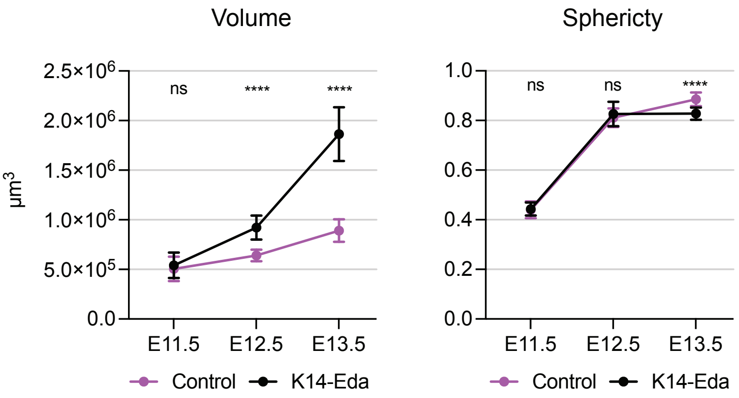

Figure 9. Quantification of mammary rudiment size and shape in K14-Eda and their control littermates' embryos in early developmental stages.

*3D surface rendering was used to analyze volume and sphericity of mammary rudiment 3 at placode ($n_{control}$=6, $n_{K14\text{-}Eda}$=4), hillock ($n_{control}$=6, $n_{K14\text{-}Eda}$=8) and bulb ($n_{control}$=11, $n_{K14\text{-}Eda}$=12) stages. Data are shown as mean ±SD. The normality of data distribution was analyzed using the Shapiro-Wilk test. Normally distributed data was analyzed using two-tailed Student's T-test. The data that failed the Shapiro-Wilk test was analyzed with the Mann-Whitney U test. **** ≤p0.0001. n indicates the number of embryos used for analysis.*

To assess if the observed volume increase in *K14-Eda* embryos is driven by cell proliferation, the data from the *K14-Eda/Fucci* mouse model was collected (Fig. 10). The inspection of the confocal images showed that similar to the wild type embryos (Publication III, Fig.

2F-G) the majority of the mammary epithelial cells were in G1/G0 phases at placode and hillock stages in *K14-Eda* embryos. A similar result was also observed in *Eda null* embryos suggesting that either loss or overexpression of Eda/NF-κB signaling pathway has no (or modest) effect on cell proliferation during early developmental stages (Fig. 10). However, this hypothesis would need to be supported by quantitative analysis of the cell cycle status including bulb stage where the largest difference in volume was observed between *K14-Eda* and control littermate embryos.

Figure 10. Cell cycle status in Eda null and K14-Eda mouse models.

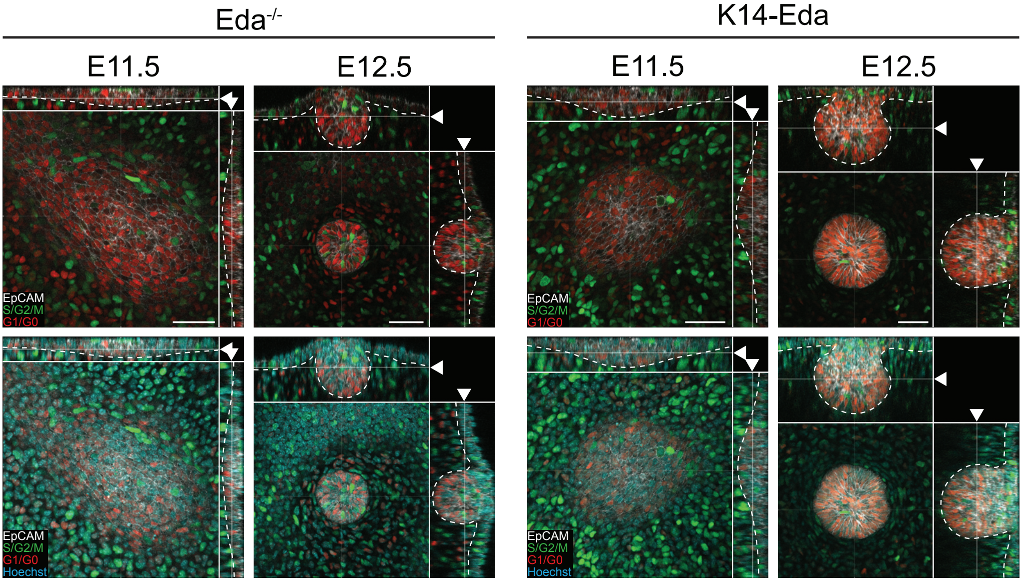

Optical sections of confocal images of mammary rudiments from Fucci cell cycle indicator in Eda null and K14-Eda background embryos stained with EpCAM (white) and Hoechst (cyan); nuclei in G1/G0 are shown in red and in S/G2/M in green (Eda null: $n_{E11.5}=2$, $n_{E12.5}=2$, K14-Eda: $n_{E11.5}=5$, $n_{E12.5}=6$). Scale bar, 50 μm. Dashed line marks the epithelial-mesenchymal border and triangle optical section.

These preliminary results indicate that Eda/NF-κB pathway does not affect cell proliferation of early mammary rudiment development but rather promotes placodal cell fate. This is in line with previous studies showing that overexpression of Eda led to enlarged hair follicles, yet no change in the cell cycle was observed (Ahtiainen et al., 2014, Mustonen et al., 2004). Interestingly, at E14.5 increased cell proliferation was reported in *K14-Eda* mammary buds, yet it was linked with Eda's function in promoting precocious branching morphogenesis (Voutilainen et al., 2012). The Eda/NF-κB pathway was shown to increase cell motility in the hair placode, and it is plausible that it exhibits similar effects on mammary epithelial cells (Ahtiainen et al., 2014). However, whether Eda stimulated increased cell motility participates only in initial stages of organogenesis and/or has impact on later developmental stages remains an open question.

4.7. EPIDERMAL KERATINOCYTES, RING CELLS, MEDIATE MAMMARY BUD INVAGINATION THROUGH ACTOMYOSIN CONTRACTILITY (III)

In the early developmental stages, mammary rudiment submerges into underlying mesenchyme in the process that is known as invagination, but how this is achieved has remained unknown.

While analyzing the EpCAM stained mammary buds in 3D, we noticed that morphological changes occur in the epidermal cells adjacent to mammary rudiment at the time when invagination is starting to take place (Fig. 11, Publication III, Fig. 4A). At the placode stage, epidermal cells bordering the mammary primordium did not differ from mammary epithelial cells. However, within 24 hours, at hillock stage, an apparent change occurred in the epidermal cells adjacent to the mammary bud: cells become elongated and thinned, aligning into a specific rim around the bud (Fig. 11). Due to their characteristic look we called them ring cells. Half a day later, at bud stage, ring cells were still visible in the epidermis, however, at bulb stage epidermal cells were again uniformly similar to the ones at placode stage. Interestingly, disappearance of ring cells from the surface epidermis was concomitant with the formation of the mammary rudiment neck at bulb stage suggesting that ring cells might contribute to the invagination. Moreover, several mammary epithelial markers such as *Fgf20*, *Bmp4*, *Lef1*, and TOP-gal show lower expression level in the neck as compared to the bud itself, indicating that the origin of these cells might be different from mammary epithelial cells (Chu et al., 2004, Hens et al., 2007, Hiremath et al., 2012).

To gain more insights into the invagination process, we analyzed the submersion of mammary primordium's top domain between E12.5 and E13.5 (Publication III, Fig. S4A). Quantification showed a significant decrease in the area in contact with epidermis throughout the invagination (Publication III, Fig. 4B). To determine if ring cells have a role in this process, we utilized whole embryo confocal imaging (Miroshnikova et al., 2018) and imaged mammary bud invagination for 5.5 hours (Publication III, Fig. 5). Similarly to *in vivo* situation, we observed a decrease in bud-epidermis contact area indicating that live imaging is recapitulating an active invagination process (Publication III, Fig. 5A-B). Analysis of cell tracks revealed that ring cells moved in a circle-like fashion, potentially generating force driving the mammary bud invagination and neck formation (Publication III, Fig. 5D).

To decipher the possible source of the force, we performed whole-mount staining of phalloidin and phosphorylated myosin light chain (pMLC) showing F-actin and active phosphorylated form of myosin, respectively (Publication III, Fig. 6A-C). Analysis of F-actin and pMLC revealed high levels of F-actin and pMLC in ring cells, particularly in those located closest to the mammary epithelial cells at hillock stage. At bud stage, high

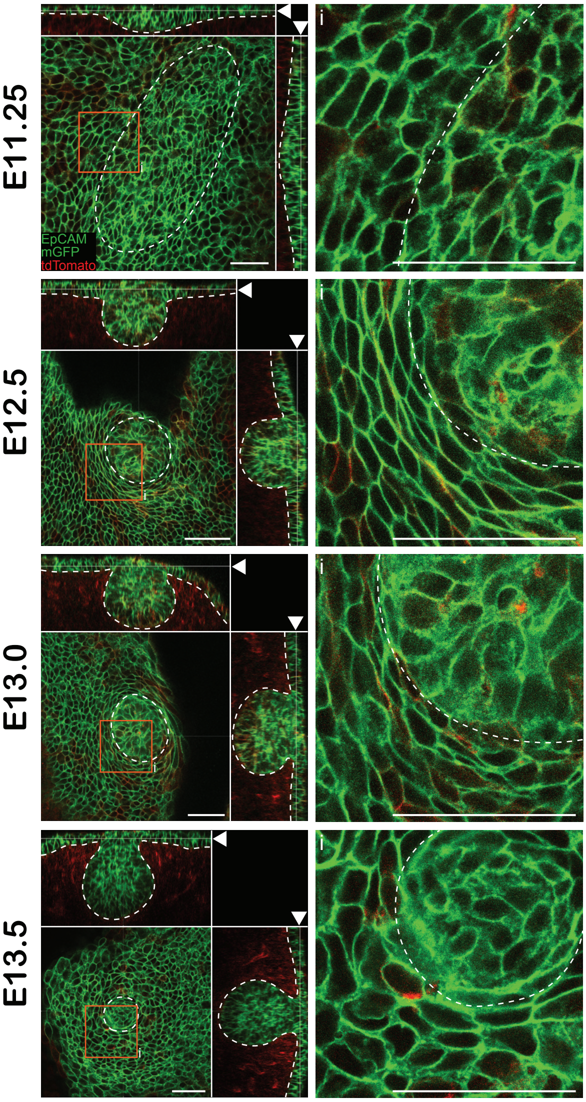

Figure 11. A rim of epidermal keratinocytes surrounds the mammary bud. *Optical sections (planar and sagittal views) of confocal whole-mount microscopy images of mammary rudiment at placode (E11.25), hillock (E12.5), bud (E13.0), and bulb (E13.5) stages. Epithelium is shown in green (mGFP and EpCAM) and mesenchyme in red. Dashed line indicates epithelial-mesenchymal border and triangle optical section. Panel on the right shows close-ups of the orange boxes. i, insert. Scale bar, 50 µm.*

intensity levels for both F-actin and pMLC persisted at the same locations where ring cells were still apparent. Disappearance of ring cells at bulb stages coincided with relatively uniform staining of both F-actin and pMLC.

To gain more insights into the role of actomyosin network in the invagination process, we chose non-muscle myosin IIA (NMIIA) as a candidate. NMIIA is the most abundantly expressed non-muscle myosin in vast range of cell types including epidermal cells (Ma et al., 2010). Quantification of NMIIA intensities showed significantly higher levels in epidermal cells than in mammary epithelial cells at both hillock and bulb stages (Publication III, Fig. 6D-E). Additionally, the expression of NMIIA persisted in neck cells at the bulb stage. Subsequently, we conditionally inactivated NMIIA by deleting *Myh9* gene (encoding the heavy chain of NMIIA), using an epithelial Cre driver, *K14-Cre*. We expected *Myh9* deletion to primarily effect ring cells since our analysis showed that NMIIA was expressed at low levels in the mammary primordium compared to epidermal keratinocytes.

To determine if loss of NMIIA has an effect on ring and epidermal cells' shape, we assessed cell roundness and aspect ratio (Publication III, Fig. 7). The quantification showed that at hillock stage in the control ring cells adjacent to the bud had higher aspect ratio and were more elongated than epidermal cells. At the same stage in *Myh9* cKO, ring cells did form, however, they were significantly less extended than in control littermates. At bulb stage, after the invagination occurred, in control embryos cells located proximally and distally to bud border had no apparent difference in shape. On the contrary, thin and elongated ring cells were still evident in *Myh9* cKO samples. Analysis of *Myh9* cKO and control samples by scanning electron microscopy revealed no difference at hillock stage between samples, however, at bulb stage *Myh9* cKO mammary buds were protruding above surface epithelium on the contrary to controls (Publication III, Fig. 9A-B). Interestingly, in *Gli3*$^{Xt\text{-}J/Xt\text{-}J}$ mammary buds often evaginate rather than invaginate and ectopic Hh signaling was reported specifically in mammary mesenchyme (Lee et al., 2011, Hatsell and Cowin, 2006). This could indicate that suppression of Hh signaling in mesenchyme is crucial for proper bud invagination. However, the role of mesenchyme in the invagination process is yet to be elucidated.

Quantification of the epidermal contact area showed a similar decreasing tendency as in controls, however it was less pronounced in all stages analyzed (Fig. 12, Publication III, Fig. 9D). The depth of the mammary bud invagination was significantly decreased in *Myh9* cKO at hillock and bud stages only (Publication III, Fig. 9E). Interestingly, there was no difference in volume between the samples indicating no general delay in mammary rudiment formation upon *Myh9* deletion (Publication III, Fig. 9F). These results demonstrated that loss of epithelial NMIIA led to diminished actomyosin contractility resulting in arrested ring cell function. As a consequence, mammary bud invagination and neck formation was impaired.

It has been previously proposed that mammary buds and other ectodermal accessory structures utilize a mechanism reported in developing teeth. In molar (cheek) teeth, the superficial cell layer of the placode intercalates forming a contractile, shrinking tissue canopy and thereby forces placodal cells to sink into the underlying mesenchyme (Panousopoulou and Green, 2016). We did not find evidence for such an organization of contractile superficial cells in intact mammary primordia. Currently, little is known about the invagination process in hair follicles, therefore, further studies are required to clarify the role of suprabasal tissue intercalation in mammary and hair buds.

This study indicates that the mammary bud invagination is driven by contractility of epidermal keratinocytes adjacent to the bud, ring cells. The model does not exclude contributions of other mechanisms and cell types supporting the invagination. One possibility is mechanical instability due to forces generated by the proliferative epidermis and non-proliferative placode being locally stabilized by the ring cells' contractility which results in invagination through a buckling-type mechanism (Nelson, 2016). It is feasible that mammary epithelial cells undergo apical constriction as suggested by their narrow apical surfaces from 3D surface renderings and expression of both *F-actin* and *pMLC*.

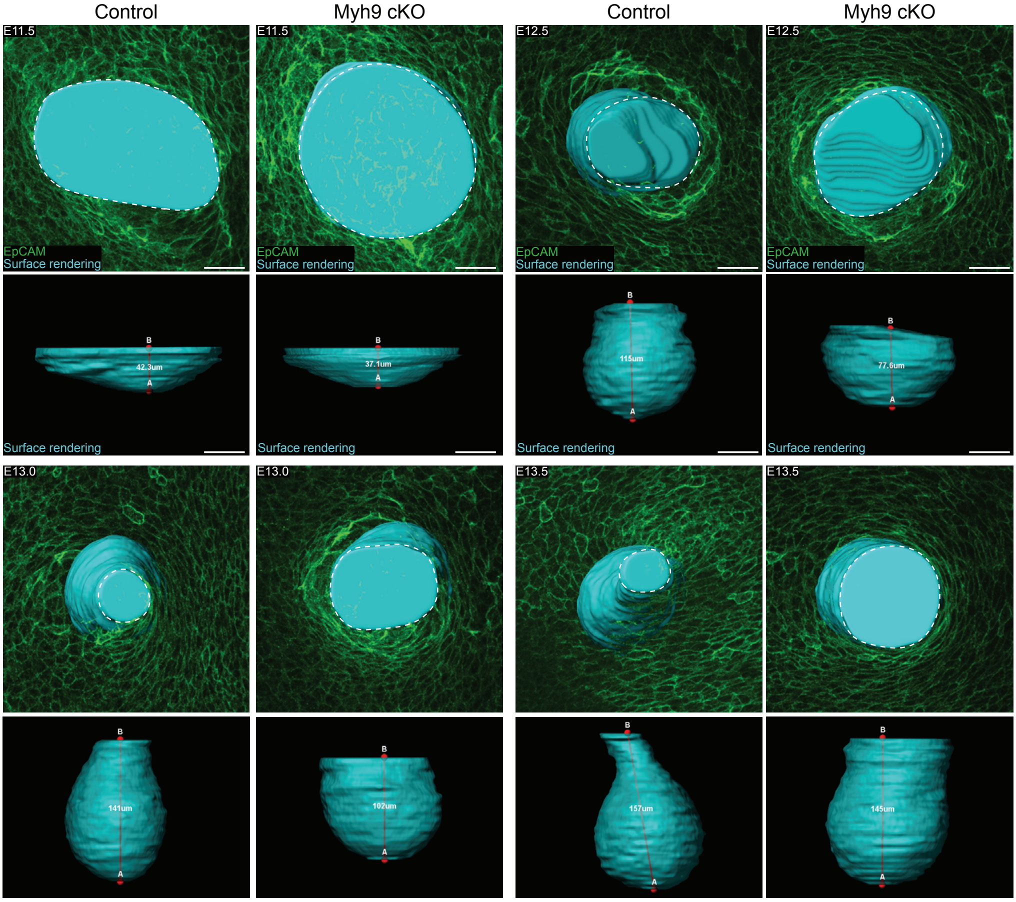

Figure 12. Loss of NMIIA to leads to impaired invagination and neck formation.
Planar and sagittal views of maximum intensity projections showing 3D surface rendering (cyan) of mammary rudiment from Myh9 cKO and control littermates embryos from placode (E11.5), hillock (E12.5), bud (E13.0), and bulb stages (E13.5). Epithelium in green (EpCAM). Dashed line indicates epidermal contact area. Red line connecting top and bottom domains of mammary primordium indicates invagination depth. Scale bar, 40 µm.

Although, we observed low expression levels of *NMIIA* in mammary epithelial cells, other NMII isoforms are known to perform both isoform-specific and isoform-redundant functions, suggesting that a different NMII isoform might function in mammary epithelial cells (Beach and Hammer, 2015, Beach et al., 2014, Shutova et al., 2014). The NMIIB is likely to act redundantly in the absence of NMIIA as both NMIIs have been shown to be expressed in mammary tissues (Nguyen-Ngoc et al., 2017). Mesenchyme is another possible contributing factor to the invagination process. In mammary rudiment, mammary mesenchyme starts to condense around it at approximately E12.5, coinciding with the onset of invagination (Propper et al., 2013). In tooth germ, mesenchyme has been shown to determine its shape through differential growth and adhesion during morphogenesis (Marin-Riera et al., 2018).

In summary, these results indicate a model in which mammary bud invagination is driven by epidermal keratinocytes, ring cells, that form a contractile rim around mammary bud and likely exert contractile force through the actomyosin network (Fig. 13). This model, however, does not exclude the possibility that other mechanisms such as intercalation canopy, apical constriction of mammary epithelial cells, buckling-type mechanism, and mesenchyme induced invagination also participate and aid in the invagination process (Fig. 13). Further studies are required to clarify the role of other mechanisms in the invagination of the mammary bud.

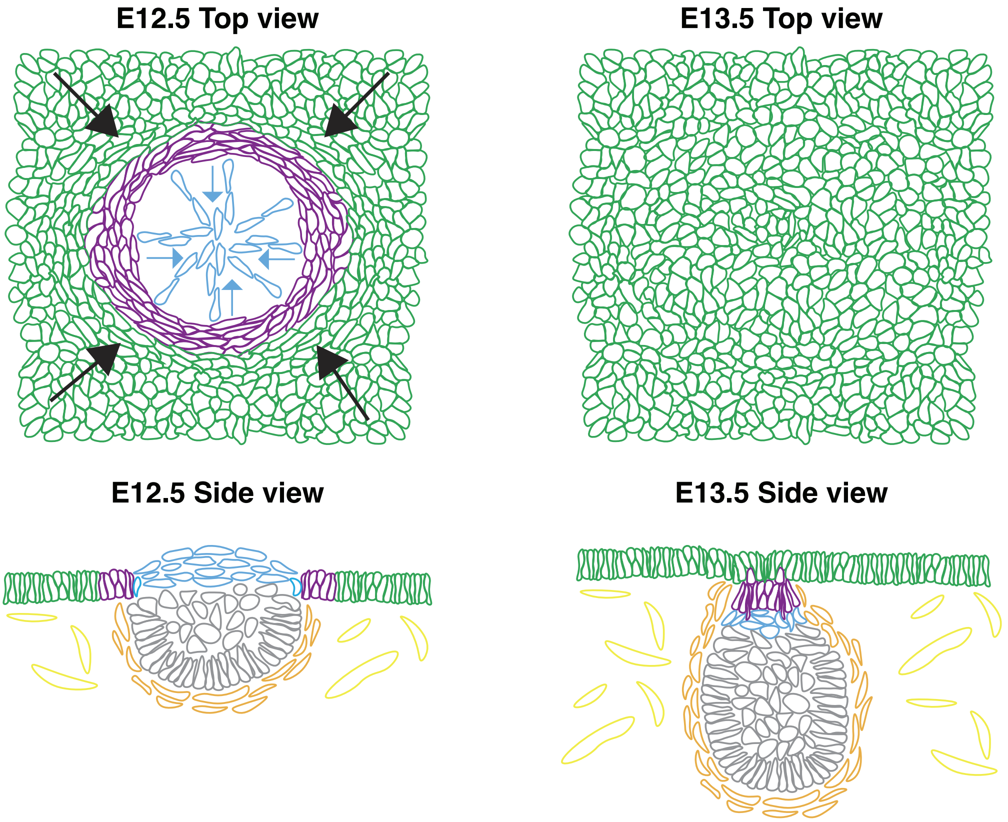

Figure 13. Schematic representation of invagination mechanism.
Ring cells (magenta), epidermal keratinocytes, appear at E12.5 creating contractile rim around mammary bud (see left top and side views). Within 24 hours ring cells disappear from epidermis (green) and are likely to constitute mammary neck cells at E13.5 (see right top and side views). It is possible, however, not studied yet, that epidermal buckling (black arrows), condensing mammary mesenchyme (orange), contractile canopy (blue), and apical constriction of mammary epithelial cells (light grey) could provide contributing forces to mammary bud invagination process. Mesenchyme shown in yellow.

5. CONCLUDING REMARKS AND FUTURE PROSPECTIVES

In mammals, the number of mammary glands differs among species. The Eda/NF-κB pathway is highly conserved in vertebrates and is known to promote placodal cell fate in several ectodermal organs including mammary glands (Mustonen et al., 2004, Mustonen et al., 2003). Considering that the number of mammary glands differs among species it is tempting to speculate that Eda/NF-κB may participate at least partly in mammary gland number specification. As revealed in this work Eda upregulates the Wnt pathway that led to the formation of ectopic mammary placodes, whereas suppression of Wnt signaling inhibited ectopic mammogenesis.

In this thesis, it has been shown that migration driven cell influx is main contributor to early mammary rudiment formation, a mechanism that has been speculated for decades (Balinsky, 1950, Balinsky, 1952, Lee et al., 2011). Having live imaging established it would be interesting to investigate the direction of cell influx into mammary placode in more detail. Currently two models have been proposed: in the first one, mammary epithelial cells migrate along milk line, and in the second one, mammary epithelial cells migrate centripetally (Propper et al., 2013). The live imaging of mammary placode reported in this thesis showed mammary epithelial cells migrated along the milk line, however, centripetal migration has not been assessed. In rabbit embryos, tracing of charcoal deposition indicated only cells from the mammary ridge contribute to mammary rudiment and not to adjacent epidermis (Propper, 1973).

Utilization of a contractile rim of epidermal keratinocytes might not be a mammary rudiment unique feature, analogous mechanism has been shown in eyelid closure (Heller et al., 2014). Similar to mammary rudiments, epidermis of eyelid front was pulled along by NMIIA dependent contraction, whereas remaining epidermal cells were passively following. This indicates that a contractile rim of epidermal keratinocytes might be a more widely used mechanism in the developmental processes.

One of the remaining open questions is what molecular signaling regulates mammary bud invagination. To date only one gene, *Sostdc1*, is known to be specifically upregulated in epidermal cells adjacent to mammary rudiment, in the location matching that of ring cells (Narhi et al., 2012). Interestingly, *Sostdc1* deletion led to abnormal mammary bud shape with a wider neck at bulb stage and coincided with misexpression of Wnt marker *Lef1*. It would be interesting to investigate if the Wnt pathway has a role in ring cell function.

In conclusion, mammary rudiment is an interesting organ to study the molecular and cellular mechanisms involved in morphogenesis. Established live imaging methods open new possibilities to study yet unanswered questions. Is cell motility increased in mammary epithelial cells upon Eda and Wnt pathway stimulation similarly to hair follicle? Are cellular mechanisms driving ectopic mammary placode formation analogous to endogenous placodes? Future studies might bring exciting results.

ACKNOWLEDGEMENTS

It is said that the acknowledgment section is the most difficult part in writing the thesis. I understand now why. It is impossible to express the gratitude to everyone who helped me, inspired me, or crossed my path during these long seven years it took to complete this thesis. It has been one of the most demanding yet incredible journeys I have taken in my entire life, and I know I would not be here without help from many people. Therefore, I would like to apologize to those who are unwittingly not mentioned here.

This thesis was carried out at the Institute of Biotechnology, University of Helsinki, HiLife with the financial support from Integrative Life Science (ILS) doctoral programme, Doctoral School in Health Sciences, Academy of Finland, the Finnish Cancer Foundation, the Sigrid Juselius Foundation, and the Center of Excellence in Experimental and Computational Developmental Biology. First and foremost, I would like to thank and express my gratitude to my supervisor Docent Marja Mikkola for seeing the potential in me on my first visit to Helsinki and giving me chance and space to become, grow and mature as scientist. Your valuable insights led me throughout these years, and I will truly miss them. I would like to extend my gratitude and appreciation to Professor Irma Thesleff. You and Marja built safe environment that was inspirational and open for scientific discussion. It was a pleasure to work in a place like that.

Throughout these years I received immense support from my thesis committee members, Docent Satu Kuure and Professor Juha Klefström. I am not only grateful for your comments and discussions during the meetings that helped me progress with my research but also for your thoughtful worries about my well-being and questions making me think about my future path. It was easier to go through these years knowing that you are there to help, if needed.

I would like to thank my pre-examiners Adjunct Professor Emilia Peuhu and Professor Aki Manninen. I am grateful you took time to read my thesis and provided me with your valuable insights and comments shaping final version of the thesis.

The work presented in this thesis would not be finalized without cooperation of many wonderful collaborators. In particular I would like to thank Professor Sara Wickström and Doctor Clémentine Villeneuve who participated in my final study. I enjoyed greatly working with you.

As a member of ILS doctoral programme I had a chance to meet other graduate students and participate in many activities that were scientific but also not so scientific oriented. I would like to express my gratitude to Doctor Erkki Raulo and Doctor Liisa Uotila for being able to create safe environment for us, students, where we could share struggles of PhD life.

Studying developmental biology meant being a part of Developmental Biology Community. I am grateful I could be one of You and share these memorable times during retreats in Tvärminne, Hyytiälä, and Pajulahti.

Everyday work was enjoyable and facing everyday struggles easier because of people who worked with me in the same floor. Mona, Maria, Solja, Meeri, Ana, Vilma, Kaisa, Sini, Roland, Irepan, Pascal, Lisandro, and many others. Thank you.

I would like to thank all members (past and present) of Mikkola group. Ana-Marija, Beata, Verdiana, Jyoti, Teresa, Vera, Leah, Vinod, Otto, and in particular Qiang, Satu, Riitta, and Vode. I could have never done it without you. Your support both in and out of the lab meant the world to me. The lab can function smoothly provided there are excellent technicians. I was lucky I met and worked with exceptional ones: Raija, Merja, Riikka and Agnes. Thank you for all help and lessons. Especially Raija, you saved me many times in the lab.

I consider myself extremely fortunate because I found a group of people with whom sharing the time outside of academia was always fun. Kasica, Jan, Paweł, Aki, Monika, Marcelina, Kamil, Patrycja, Łukasz, Katarzyna, Magda, Marko, Asia, Magda, Emilia, Wojtek, Giulio, Arvydas, and Behnam. Thank you for all the memories.

Life has its ups and downs. It gets tough sometimes especially if you live and pursue the doctoral degree abroad. However, if you are lucky and find those people who will constitute your "other" family there is nothing you can fear with support like that. For me it is Emily, Alison and Isa.

I would like to thank my family. Romanie, Bogno, Asiu, Haniu, mamo i tato bez Was, Waszej wiary we mnie i miłości nie byłabym tu, gdzie jestem dzisiaj. Nie mogłabym prosić o lepszą rodzinę. Dziękuję za to, że jesteście i wspieraliście mnie przez te wszystkie lata.

Konrad whenever I have my hand in your palm and I feel you are next to me, I am not afraid of anything because I know we can sustain any storm. It was you who kept me sane throughout this time. I love you 3000.

Helsinki 2021

Ewelina Trela

REFERENCES

Ahn, Y., Sims, C., Logue, J. M., Weatherbee, S. D. & Krumlauf, R. 2013. Lrp4 and Wise interplay controls the formation and patterning of mammary and other skin appendage placodes by modulating Wnt signaling. *Development,* 140**,** 583-93.

Ahtiainen, L., Lefebvre, S., Lindfors, P. H., Renvoise, E., Shirokova, V., Vartiainen, M. K., Thesleff, I. & Mikkola, M. L. 2014. Directional cell migration, but not proliferation, drives hair placode morphogenesis. *Dev Cell,* 28**,** 588-602.

Ahtiainen, L., Uski, I., Thesleff, I. & Mikkola, M. L. 2016. Early epithelial signaling center governs tooth budding morphogenesis. *J Cell Biol,* 214**,** 753-67.

Andl, T., Ahn, K., Kairo, A., Chu, E. Y., Wine-Lee, L., Reddy, S. T., Croft, N. J., Cebra-Thomas, J. A., Metzger, D., Chambon, P., Lyons, K. M., Mishina, Y., Seykora, J. T., Crenshaw, E. B., 3rd & Millar, S. E. 2004. Epithelial Bmpr1a regulates differentiation and proliferation in postnatal hair follicles and is essential for tooth development. *Development,* 131**,** 2257-68.

Andl, T., Reddy, S. T., Gaddapara, T. & Millar, S. E. 2002. WNT signals are required for the initiation of hair follicle development. *Dev Cell,* 2**,** 643-53.

Arte, S., Parmanen, S., Pirinen, S., Alaluusua, S. & Nieminen, P. 2013. Candidate gene analysis of tooth agenesis identifies novel mutations in six genes and suggests significant role for WNT and EDA signaling and allele combinations. *PLoS One,* 8**,** e73705.

Arteaga, C. L. & Engelman, J. A. 2014. ERBB receptors: from oncogene discovery to basic science to mechanism-based cancer therapeutics. *Cancer Cell,* 25**,** 282-303.

Bal, E., Baala, L., Cluzeau, C., El Kerch, F., Ouldim, K., Hadj-Rabia, S., Bodemer, C., Munnich, A., Courtois, G., Sefiani, A. & Smahi, A. 2007. Autosomal dominant anhidrotic ectodermal dysplasias at the EDARADD locus. *Hum Mutat,* 28**,** 703-9.

Balinsky, B. I. 1950. On the prenatal growth of the mammary gland rudiment in the mouse. *J Anat,* 84**,** 227-35.

Balinsky, B. I. 1952. I.—On the Developmental Processes in Mammary Glands and other Epidermal Structures. *Transactions of the Royal Society of Edinburgh,* 62**,** 1-31.

Barak, H., Huh, S. H., Chen, S., Jeanpierre, C., Martinovic, J., Parisot, M., Bole-Feysot, C., Nitschke, P., Salomon, R., Antignac, C., Ornitz, D. M. & Kopan, R. 2012. FGF9 and FGF20 maintain the stemness of nephron progenitors in mice and man. *Dev Cell,* 22**,** 1191-207.

Beach, J. R. & Hammer, J. A., 3rd 2015. Myosin II isoform co-assembly and differential regulation in mammalian systems. *Exp Cell Res,* 334**,** 2-9.

Beach, J. R., Shao, L., Remmert, K., Li, D., Betzig, E. & Hammer, J. A., 3rd 2014. Nonmuscle myosin II isoforms coassemble in living cells. *Curr Biol,* 24**,** 1160-6.

Benhaj, K., Akcali, K. C. & Ozturk, M. 2006. Redundant expression of canonical Wnt ligands in human breast cancer cell lines. *Oncol Rep,* 15**,** 701-7.

Bhakar, A. L., Tannis, L. L., Zeindler, C., Russo, M. P., Jobin, C., Park, D. S., Macpherson, S. & Barker, P. A. 2002. Constitutive nuclear factor-kappa B activity is required for central neuron survival. *J Neurosci,* 22**,** 8466-75.

Bianchi, N., Depianto, D., Mcgowan, K., Gu, C. & Coulombe, P. A. 2005. Exploiting the keratin 17 gene promoter to visualize live cells in epithelial appendages of mice. *Mol Cell Biol,* 25**,** 7249-59.

Biggs, L. C. & Mikkola, M. L. 2014. Early inductive events in ectodermal appendage morphogenesis. *Semin Cell Dev Biol,* 25-26**,** 11-21.

Boras-Granic, K. & Hamel, P. A. 2013. Wnt-signalling in the embryonic mammary gland. *J Mammary Gland Biol Neoplasia,* 18**,** 155-63.

Bray, F., Ferlay, J., Soerjomataram, I., Siegel, R. L., Torre, L. A. & Jemal, A. 2018. Global cancer statistics 2018: GLOBOCAN estimates of incidence and mortality worldwide for 36 cancers in 185 countries. *CA Cancer J Clin,* 68**,** 394-424.

Brisken, C. 2002. Hormonal control of alveolar development and its implications for breast carcinogenesis. *J Mammary Gland Biol Neoplasia,* 7**,** 39-48.

Budi, E. H., Duan, D. & Derynck, R. 2017. Transforming Growth Factor-beta Receptors and Smads: Regulatory Complexity and Functional Versatility. *Trends Cell Biol,* 27**,** 658-672.

Butti, R., Gunasekaran, V. P., Kumar, T. V. S., Banerjee, P. & Kundu, G. C. 2019. Breast cancer stem cells: Biology and therapeutic implications. *Int J Biochem Cell Biol,* 107**,** 38-52.

Byrne, C., Tainsky, M. & Fuchs, E. 1994. Programming gene expression in developing epidermis. *Development,* 120**,** 2369-83.

Callahan, R. 1996. MMTV-induced mutations in mouse mammary tumors: their potential relevance to human breast cancer. *Breast Cancer Res Treat,* 39**,** 33-44.

Carroll, L. S. & Capecchi, M. R. 2015. Hoxc8 initiates an ectopic mammary program by regulating Fgf10 and Tbx3 expression and Wnt/beta-catenin signaling. *Development,* 142**,** 4056-67.

Chang, S. H., Jobling, S., Brennan, K. & Headon, D. J. 2009. Enhanced Edar signalling has pleiotropic effects on craniofacial and cutaneous glands. *PLoS One,* 4**,** e7591.

Chassaing, N., Bourthoumieu, S., Cossee, M., Calvas, P. & Vincent, M. C. 2006. Mutations in EDAR account for one-quarter of non-ED1-related hypohidrotic ectodermal dysplasia. *Hum Mutat,* 27**,** 255-9.

Chauhan, V. P., Chen, I. X., Tong, R., Ng, M. R., Martin, J. D., Naxerova, K., Wu, M. W., Huang, P., Boucher, Y., Kohane, D. S., Langer, R. & Jain, R. K. 2019. Reprogramming the microenvironment with tumor-selective angiotensin blockers enhances cancer immunotherapy. *Proc Natl Acad Sci U S A,* 116**,** 10674-10680.

Cho, K. W., Kim, J. Y., Song, S. J., Farrell, E., Eblaghie, M. C., Kim, H. J., Tickle, C. & Jung, H. S. 2006. Molecular interactions between Tbx3 and Bmp4 and a model for dorsoventral positioning of mammary gland development. *Proc Natl Acad Sci U S A,* 103**,** 16788-93.

Christiansen, J. H., Dennis, C. L., Wicking, C. A., Monkley, S. J., Wilkinson, D. G. & Wainwright, B. J. 1995. Murine Wnt-11 and Wnt-12 have temporally and spatially restricted expression patterns during embryonic development. *Mech Dev,* 51**,** 341-50.

Chu, E. Y., Hens, J., Andl, T., Kairo, A., Yamaguchi, T. P., Brisken, C., Glick, A., Wysolmerski, J. J. & Millar, S. E. 2004. Canonical WNT signaling promotes mammary placode development and is essential for initiation of mammary gland morphogenesis. *Development,* 131**,** 4819-29.

Chugh, P. & Paluch, E. K. 2018. The actin cortex at a glance. *J Cell Sci,* 131.

Chuong, C.-M. 1998. *Molecular basis of epithelial appendage morphogenesis*, Landes Bioscience.

Clarke, A., Phillips, D. I., Brown, R. & Harper, P. S. 1987. Clinical aspects of X-linked hypohidrotic ectodermal dysplasia. *Arch Dis Child,* 62**,** 989-96.

Cui, C. Y., Yin, M., Sima, J., Childress, V., Michel, M., Piao, Y. & Schlessinger, D. 2014. Involvement of Wnt, Eda and Shh at defined stages of sweat gland development. *Development,* 141**,** 3752-60.

Cunha, G. R., Young, P., Christov, K., Guzman, R., Nandi, S., Talamantes, F. & Thordarson, G. 1995. Mammary phenotypic expression induced in epidermal cells by embryonic mammary mesenchyme. *Acta Anat (Basel),* 152**,** 195-204.

Dasgupta, R. & Fuchs, E. 1999. Multiple roles for activated LEF/TCF transcription complexes during hair follicle development and differentiation. *Development,* 126**,** 4557-68.

Dassule, H. R. & Mcmahon, A. P. 1998. Analysis of epithelial-mesenchymal interactions in the initial morphogenesis of the mammalian tooth. *Dev Biol,* 202**,** 215-27.

Davenport, T. G., Jerome-Majewska, L. A. & Papaioannou, V. E. 2003. Mammary gland, limb and yolk sac defects in mice lacking Tbx3, the gene mutated in human ulnar mammary syndrome. *Development,* 130**,** 2263-73.

Decosse, J. J., Gossens, C. L., Kuzma, J. F. & Unsworth, B. R. 1973. Breast cancer: induction of differentiation by embryonic tissue. *Science,* 181**,** 1057-8.

Deome, K. B., Faulkin, L. J., Jr., Bern, H. A. & Blair, P. B. 1959. Development of mammary tumors from hyperplastic alveolar nodules transplanted into gland-free mammary fat pads of female C3H mice. *Cancer Res,* 19**,** 515-20.

Dontu, G. & Ince, T. A. 2015. Of mice and women: a comparative tissue biology perspective of breast stem cells and differentiation. *J Mammary Gland Biol Neoplasia,* 20**,** 51-62.

Drews, U. & Drews, U. 1977. Regression of mouse mammary gland anlagen in recombinants of Tfm and wild-type tissues: testosterone acts via the mesenchyme. *Cell,* 10**,** 401-4.

Driever, W. & Nusslein-Volhard, C. 1988. The bicoid protein determines position in the Drosophila embryo in a concentration-dependent manner. *Cell,* 54**,** 95-104.

Dunbar, M. E., Dann, P. R., Robinson, G. W., Hennighausen, L., Zhang, J. P. & Wysolmerski, J. J. 1999. Parathyroid hormone-related protein signaling is necessary for sexual dimorphism during embryonic mammary development. *Development,* 126**,** 3485-93.

Duverger, O. & Morasso, M. I. 2008. Role of homeobox genes in the patterning, specification, and differentiation of ectodermal appendages in mammals. *J Cell Physiol,* 216**,** 337-46.

Eblaghie, M. C., Song, S. J., Kim, J. Y., Akita, K., Tickle, C. & Jung, H. S. 2004. Interactions between FGF and Wnt signals and Tbx3 gene expression in mammary gland initiation in mouse embryos. *J Anat,* 205**,** 1-13.

Falconer, D. S. 1952. A totally sex-linked gene in the house mouse. *Nature,* 169**,** 664-5.

Faulkin, L. J., Jr. & Deome, K. B. 1960. Regulation of growth and spacing of gland elements in the mammary fat pad of the C3H mouse. *J Natl Cancer Inst,* 24**,** 953-69.

Fliniaux, I., Mikkola, M. L., Lefebvre, S. & Thesleff, I. 2008. Identification of dkk4 as a target of Eda-A1/Edar pathway reveals an unexpected role of ectodysplasin as inhibitor of Wnt signalling in ectodermal placodes. *Dev Biol,* 320**,** 60-71.

Foley, J., Dann, P., Hong, J., Cosgrove, J., Dreyer, B., Rimm, D., Dunbar, M., Philbrick, W. & Wysolmerski, J. 2001. Parathyroid hormone-related protein maintains mammary epithelial fate and triggers nipple skin differentiation during embryonic breast development. *Development,* 128**,** 513-25.

Friedl, P., Wolf, K. & Lammerding, J. 2011. Nuclear mechanics during cell migration. *Curr Opin Cell Biol,* 23**,** 55-64.

Fu, N. Y., Nolan, E., Lindeman, G. J. & Visvader, J. E. 2020. Stem Cells and the Differentiation Hierarchy in Mammary Gland Development. *Physiol Rev,* 100**,** 489-523.

Gallego, M. I., Binart, N., Robinson, G. W., Okagaki, R., Coschigano, K. T., Perry, J., Kopchick, J. J., Oka, T., Kelly, P. A. & Hennighausen, L. 2001. Prolactin, growth hormone, and epidermal growth factor activate Stat5 in different compartments of mammary tissue and exert different and overlapping developmental effects. *Dev Biol,* 229**,** 163-75.

Garcia-Gasca, A. & Spyropoulos, D. D. 2000. Differential mammary morphogenesis along the anteroposterior axis in Hoxc6 gene targeted mice. *Dev Dyn,* 219**,** 261-76.

Gilbert, S. 2014. *Developmental biology, 10th Edition,* Sunderland (MA), Sinauer Associates, Inc.

Gillard, G. & Roper, K. 2020. Control of cell shape during epithelial morphogenesis: recent advances. *Curr Opin Genet Dev,* 63**,** 1-8.

Gregory, W. K. 1910. *The orders of mammals*, The Trustees.

Gu, B., Sun, P., Yuan, Y., Moraes, R. C., Li, A., Teng, A., Agrawal, A., Rheaume, C., Bilanchone, V., Veltmaat, J. M., Takemaru, K., Millar, S., Lee, E. Y., Lewis, M. T., Li, B. & Dai, X. 2009. Pygo2 expands mammary progenitor cells by facilitating histone H3 K4 methylation. *J Cell Biol,* 185**,** 811-26.

Guillot, C. & Lecuit, T. 2013. Mechanics of epithelial tissue homeostasis and morphogenesis. *Science,* 340**,** 1185-9.

Haara, O., Harjunmaa, E., Lindfors, P. H., Huh, S. H., Fliniaux, I., Aberg, T., Jernvall, J., Ornitz, D. M., Mikkola, M. L. & Thesleff, I. 2012. Ectodysplasin regulates activator-inhibitor balance in murine tooth development through Fgf20 signaling. *Development,* 139**,** 3189-99.

Hafner, M., Wenk, J., Nenci, A., Pasparakis, M., Scharffetter-Kochanek, K., Smyth, N., Peters, T., Kess, D., Holtkotter, O., Shephard, P., Kudlow, J. E., Smola, H., Haase, I., Schippers, A., Krieg, T. & Muller, W. 2004. Keratin 14 Cre transgenic mice authenticate keratin 14 as an oocyte-expressed protein. *Genesis,* 38**,** 176-81.

Haghighi, A., Nikuei, P., Haghighi-Kakhki, H., Saleh-Gohari, N., Baghestani, S., Krawitz, P. M., Hecht, J. & Mundlos, S. 2013. Whole-exome sequencing identifies a novel missense mutation in EDAR causing autosomal recessive hypohidrotic ectodermal dysplasia with bilateral amastia and palmoplantar hyperkeratosis. *Br J Dermatol,* 168**,** 1353-6.

Hatsell, S. J. & Cowin, P. 2006. Gli3-mediated repression of Hedgehog targets is required for normal mammary development. *Development,* 133**,** 3661-70.

Headon, D. J., Emmal, S. A., Ferguson, B. M., Tucker, A. S., Justice, M. J., Sharpe, P. T., Zonana, J. & Overbeek, P. A. 2001. Gene defect in ectodermal dysplasia implicates a death domain adapter in development. *Nature,* 414**,** 913-6.

Headon, D. J. & Overbeek, P. A. 1999. Involvement of a novel Tnf receptor homologue in hair follicle induction. *Nat Genet,* 22**,** 370-4.

Heisenberg, C. P. & Bellaiche, Y. 2013. Forces in tissue morphogenesis and patterning. *Cell,* 153**,** 948-62.

Heller, E., Kumar, K. V., Grill, S. W. & Fuchs, E. 2014. Forces generated by cell intercalation tow epidermal sheets in mammalian tissue morphogenesis. *Dev Cell,* 28**,** 617-32.

Hens, J. R., Dann, P., Zhang, J. P., Harris, S., Robinson, G. W. & Wysolmerski, J. 2007. BMP4 and PTHrP interact to stimulate ductal outgrowth during embryonic mammary development and to inhibit hair follicle induction. *Development,* 134**,** 1221-30.

Heuberger, B., Fitzka, I., Wasner, G. & Kratochwil, K. 1982. Induction of androgen receptor formation by epithelium-mesenchyme interaction in embryonic mouse mammary gland. *Proc Natl Acad Sci U S A,* 79**,** 2957-61.

Hiremath, M., Dann, P., Fischer, J., Butterworth, D., Boras-Granic, K., Hens, J., Van Houten, J., Shi, W. & Wysolmerski, J. 2012. Parathyroid hormone-related protein activates Wnt signaling to specify the embryonic mammary mesenchyme. *Development,* 139**,** 4239-49.

Hogg, N. A., Harrison, C. J. & Tickle, C. 1983. Lumen formation in the developing mouse mammary gland. *J Embryol Exp Morphol,* 73**,** 39-57.

Hohmann, T. & Dehghani, F. 2019. The Cytoskeleton-A Complex Interacting Meshwork. *Cells,* 8.

Holland, P. W., Booth, H. A. & Bruford, E. A. 2007. Classification and nomenclature of all human homeobox genes. *BMC Biol,* 5**,** 47.

Howard, B. & Ashworth, A. 2006. Signalling pathways implicated in early mammary gland morphogenesis and breast cancer. *PLoS Genet,* 2**,** e112.

Howard, B., Panchal, H., Mccarthy, A. & Ashworth, A. 2005. Identification of the scaramanga gene implicates Neuregulin3 in mammary gland specification. *Genes Dev,* 19**,** 2078-90.

Howard, B. A. & Lu, P. 2014. Stromal regulation of embryonic and postnatal mammary epithelial development and differentiation. *Semin Cell Dev Biol,* 25-26**,** 43-51.

Hu, A. & Song, B. L. 2019. The interplay of Patched, Smoothened and cholesterol in Hedgehog signaling. *Curr Opin Cell Biol,* 61**,** 31-38.

Huang, S. M., Mishina, Y. M., Liu, S., Cheung, A., Stegmeier, F., Michaud, G. A., Charlat, O., Wiellette, E., Zhang, Y., Wiessner, S., Hild, M., Shi, X., Wilson, C. J., Mickanin, C., Myer, V., Fazal, A., Tomlinson, R., Serluca, F., Shao, W., Cheng, H., Shultz, M., Rau, C., Schirle, M., Schlegl, J., Ghidelli, S., Fawell, S., Lu, C., Curtis, D., Kirschner, M. W., Lengauer, C., Finan, P. M., Tallarico, J. A., Bouwmeester, T., Porter, J. A., Bauer, A. & Cong, F. 2009. Tankyrase inhibition stabilizes axin and antagonizes Wnt signalling. *Nature,* 461**,** 614-20.

Huh, S. H., Jones, J., Warchol, M. E. & Ornitz, D. M. 2012. Differentiation of the lateral compartment of the cochlea requires a temporally restricted FGF20 signal. *PLoS Biol,* 10**,** e1001231.

Huh, S. H., Narhi, K., Lindfors, P. H., Haara, O., Yang, L., Ornitz, D. M. & Mikkola, M. L. 2013. Fgf20 governs formation of primary and secondary dermal condensations in developing hair follicles. *Genes Dev,* 27**,** 450-8.

Huh, S. H., Warchol, M. E. & Ornitz, D. M. 2015. Cochlear progenitor number is controlled through mesenchymal FGF receptor signaling. *Elife,* 4.

Inman, J. L., Robertson, C., Mott, J. D. & Bissell, M. J. 2015. Mammary gland development: cell fate specification, stem cells and the microenvironment. *Development,* 142**,** 1028-42.

Itin, P. H. & Fistarol, S. K. 2004. Ectodermal dysplasias. *Am J Med Genet C Semin Med Genet,* 131C**,** 45-51.

Jerome-Majewska, L. A., Jenkins, G. P., Ernstoff, E., Zindy, F., Sherr, C. J. & Papaioannou, V. E. 2005. Tbx3, the ulnar-mammary syndrome gene, and Tbx2 interact in mammary gland development through a p19Arf/p53-independent pathway. *Dev Dyn,* 234**,** 922-33.

Kamberov, Y. G., Wang, S., Tan, J., Gerbault, P., Wark, A., Tan, L., Yang, Y., Li, S., Tang, K., Chen, H., Powell, A., Itan, Y., Fuller, D., Lohmueller, J., Mao, J., Schachar, A., Paymer, M., Hostetter, E., Byrne, E., Burnett, M., Mcmahon, A. P., Thomas, M. G., Lieberman, D. E., Jin, L., Tabin, C. J., Morgan, B. A. & Sabeti, P. C. 2013. Modeling recent human evolution in mice by expression of a selected EDAR variant. *Cell,* 152**,** 691-702.

Kere, J., Srivastava, A. K., Montonen, O., Zonana, J., Thomas, N., Ferguson, B., Munoz, F., Morgan, D., Clarke, A., Baybayan, P., Chen, E. Y., Ezer, S., Saarialho-Kere, U., De La Chapelle, A. & Schlessinger, D. 1996. X-linked anhidrotic (hypohidrotic) ectodermal dysplasia is caused by mutation in a novel transmembrane protein. *Nat Genet,* 13**,** 409-16.

Kogata, N., Bland, P., Tsang, M., Oliemuller, E., Lowe, A. & Howard, B. A. 2018. Sox9 regulates cell state and activity of embryonic mouse mammary progenitor cells. *Commun Biol,* 1**,** 228.

Kogata, N., Oliemuller, E., Wansbury, O. & Howard, B. A. 2014. Neuregulin-3 regulates epithelial progenitor cell positioning and specifies mammary phenotype. *Stem Cells Dev,* 23**,** 2758-70.

Kondo, S. & Miura, T. 2010. Reaction-diffusion model as a framework for understanding biological pattern formation. *Science,* 329**,** 1616-20.

Kowalczyk-Quintas, C. & Schneider, P. 2014. Ectodysplasin A (EDA) - EDA receptor signalling and its pharmacological modulation. *Cytokine Growth Factor Rev,* 25**,** 195-203.

Kratochwil, K. 1969. Organ specificity in mesenchymal induction demonstrated in the embryonic development of the mammary gland of the mouse. *Dev Biol,* 20**,** 46-71.

Kratochwil, K. 1977. Development and loss of androgen responsiveness in the embryonic rudiment of the mouse mammary gland. *Dev Biol,* 61**,** 358-65.

Kratochwil, K. & Schwartz, P. 1976. Tissue interaction in androgen response of embryonic mammary rudiment of mouse: identification of target tissue for testosterone. *Proc Natl Acad Sci U S A,* 73**,** 4041-4.

Kreuzaler, P. A., Staniszewska, A. D., Li, W., Omidvar, N., Kedjouar, B., Turkson, J., Poli, V., Flavell, R. A., Clarkson, R. W. & Watson, C. J. 2011. Stat3 controls lysosomal-mediated cell death in vivo. *Nat Cell Biol,* 13**,** 303-9.

Laurikkala, J., Mikkola, M., Mustonen, T., Aberg, T., Koppinen, P., Pispa, J., Nieminen, P., Galceran, J., Grosschedl, R. & Thesleff, I. 2001. TNF signaling via the ligand-receptor pair ectodysplasin and edar controls the function of epithelial signaling centers and is regulated by Wnt and activin during tooth organogenesis. *Dev Biol,* 229**,** 443-55.

Laurikkala, J., Pispa, J., Jung, H. S., Nieminen, P., Mikkola, M., Wang, X., Saarialho-Kere, U., Galceran, J., Grosschedl, R. & Thesleff, I. 2002. Regulation of hair follicle development by the TNF signal ectodysplasin and its receptor Edar. *Development,* 129**,** 2541-53.

Lecuit, T. & Lenne, P. F. 2007. Cell surface mechanics and the control of cell shape, tissue patterns and morphogenesis. *Nat Rev Mol Cell Biol,* 8**,** 633-44.

Lecuit, T., Lenne, P. F. & Munro, E. 2011. Force generation, transmission, and integration during cell and tissue morphogenesis. *Annu Rev Cell Dev Biol,* 27**,** 157-84.

Lee, M. Y., Racine, V., Jagadpramana, P., Sun, L., Yu, W., Du, T., Spencer-Dene, B., Rubin, N., Le, L., Ndiaye, D., Bellusci, S., Kratochwil, K. & Veltmaat, J. M. 2011. Ectodermal influx and cell hypertrophy provide early growth for all murine mammary rudiments, and are differentially regulated among them by Gli3. *PLoS One,* 6**,** e26242.

Lee, R. T., Zhao, Z. & Ingham, P. W. 2016. Hedgehog signalling. *Development,* 143**,** 367-72.

Lefebvre, S., Fliniaux, I., Schneider, P. & Mikkola, M. L. 2012. Identification of ectodysplasin target genes reveals the involvement of chemokines in hair development. *J Invest Dermatol,* 132**,** 1094-102.

Lehtimaki, J., Hakala, M. & Lappalainen, P. 2017. Actin Filament Structures in Migrating Cells. *Handb Exp Pharmacol,* 235**,** 123-152.

Leon, C., Eckly, A., Hechler, B., Aleil, B., Freund, M., Ravanat, C., Jourdain, M., Nonne, C., Weber, J., Tiedt, R., Gratacap, M. P., Severin, S., Cazenave, J. P., Lanza, F., Skoda, R. & Gachet, C. 2007. Megakaryocyte-restricted MYH9 inactivation dramatically affects hemostasis while preserving platelet aggregation and secretion. *Blood,* 110**,** 3183-91.

Lindfors, P. H., Voutilainen, M. & Mikkola, M. L. 2013. Ectodysplasin/NF-kappaB signaling in embryonic mammary gland development. *J Mammary Gland Biol Neoplasia,* 18**,** 165-9.

Lindvall, C., Evans, N. C., Zylstra, C. R., Li, Y., Alexander, C. M. & Williams, B. O. 2006. The Wnt signaling receptor Lrp5 is required for mammary ductal stem cell activity and Wnt1-induced tumorigenesis. *J Biol Chem,* 281**,** 35081-7.

Lindvall, C., Zylstra, C. R., Evans, N., West, R. A., Dykema, K., Furge, K. A. & Williams, B. O. 2009. The Wnt co-receptor Lrp6 is required for normal mouse mammary gland development. *PLoS One,* 4**,** e5813.

Linné, C. V. 1789. *Systema naturae per regna tria naturae: secundum classes, ordines, genera, species, cum characteribus, differentiis, synonymis, locis. Vol. 1, pt. 7,* Lugduni: Apud JB Delamolliere.

M'boneko, V. & Merker, H. J. 1988. Development and morphology of the periderm of mouse embryos (days 9-12 of gestation). *Acta Anat (Basel),* 133**,** 325-36.

Ma, X., Jana, S. S., Conti, M. A., Kawamoto, S., Claycomb, W. C. & Adelstein, R. S. 2010. Ablation of nonmuscle myosin II-B and II-C reveals a role for nonmuscle myosin II in cardiac myocyte karyokinesis. *Mol Biol Cell,* 21**,** 3952-62.

Macias, H. & Hinck, L. 2012. Mammary gland development. *Wiley Interdiscip Rev Dev Biol,* 1**,** 533-57.

Mahler, B., Gocken, T., Brojan, M., Childress, S., Spandau, D. F. & Foley, J. 2004. Keratin 2e: a marker for murine nipple epidermis. *Cells Tissues Organs,* 176**,** 169-77.

Mailleux, A. A., Spencer-Dene, B., Dillon, C., Ndiaye, D., Savona-Baron, C., Itoh, N., Kato, S., Dickson, C., Thiery, J. P. & Bellusci, S. 2002. Role of FGF10/FGFR2b signaling during mammary gland development in the mouse embryo. *Development,* 129**,** 53-60.

Majumder, K., Shawlot, W., Schuster, G., Harrison, W., Elder, F. F. & Overbeek, P. A. 1998. YAC rescue of downless locus mutations in mice. *Mamm Genome,* 9**,** 863-8.

Marin-Riera, M., Moustakas-Verho, J., Savriama, Y., Jernvall, J. & Salazar-Ciudad, I. 2018. Differential tissue growth and cell adhesion alone drive early tooth morphogenesis: An ex vivo and in silico study. *PLoS Comput Biol,* 14**,** e1005981.

Martin, A. C. & Goldstein, B. 2014. Apical constriction: themes and variations on a cellular mechanism driving morphogenesis. *Development,* 141**,** 1987-98.

Mccauley, L. K. & Martin, T. J. 2012. Twenty-five years of PTHrP progress: from cancer hormone to multifunctional cytokine. *J Bone Miner Res,* 27**,** 1231-9.

Mcnally, S. & Stein, T. 2017. Overview of Mammary Gland Development: A Comparison of Mouse and Human. *Methods Mol Biol,* 1501**,** 1-17.

Megarbane, H., Cluzeau, C., Bodemer, C., Fraitag, S., Chababi-Atallah, M., Megarbane, A. & Smahi, A. 2008. Unusual presentation of a severe autosomal recessive anhydrotic ectodermal dysplasia with a novel mutation in the EDAR gene. *Am J Med Genet A,* 146A**,** 2657-62.

Mikkola, M. L. 2007. Genetic basis of skin appendage development. *Semin Cell Dev Biol,* 18**,** 225-36.

Mikkola, M. L. 2008. TNF superfamily in skin appendage development. *Cytokine Growth Factor Rev,* 19**,** 219-30.

Mikkola, M. L. 2009. Molecular aspects of hypohidrotic ectodermal dysplasia. *Am J Med Genet A,* 149A**,** 2031-6.

Mikkola, M. L. & Millar, S. E. 2006. The mammary bud as a skin appendage: unique and shared aspects of development. *J Mammary Gland Biol Neoplasia,* 11**,** 187-203.

Miroshnikova, Y. A., Le, H. Q., Schneider, D., Thalheim, T., Rubsam, M., Bremicker, N., Polleux, J., Kamprad, N., Tarantola, M., Wang, I., Balland, M., Niessen, C. M., Galle, J. & Wickstrom, S. A. 2018. Adhesion forces and cortical tension couple cell proliferation and differentiation to drive epidermal stratification. *Nat Cell Biol,* 20**,** 69-80.

Monreal, A. W., Ferguson, B. M., Headon, D. J., Street, S. L., Overbeek, P. A. & Zonana, J. 1999. Mutations in the human homologue of mouse dl cause autosomal recessive and dominant hypohidrotic ectodermal dysplasia. *Nat Genet,* 22**,** 366-9.

Mou, C., Thomason, H. A., Willan, P. M., Clowes, C., Harris, W. E., Drew, C. F., Dixon, J., Dixon, M. J. & Headon, D. J. 2008. Enhanced ectodysplasin-A receptor (EDAR) signaling alters multiple fiber characteristics to produce the East Asian hair form. *Hum Mutat,* 29**,** 1405-11.

Mueller, T. D. & Nickel, J. 2012. Promiscuity and specificity in BMP receptor activation. *FEBS Lett,* 586**,** 1846-59.

Munjal, A. & Lecuit, T. 2014. Actomyosin networks and tissue morphogenesis. *Development,* 141**,** 1789-93.

Mustonen, T., Ilmonen, M., Pummila, M., Kangas, A. T., Laurikkala, J., Jaatinen, R., Pispa, J., Gaide, O., Schneider, P., Thesleff, I. & Mikkola, M. L. 2004. Ectodysplasin A1 promotes placodal cell fate during early morphogenesis of ectodermal appendages. *Development,* 131**,** 4907-19.

Mustonen, T., Pispa, J., Mikkola, M. L., Pummila, M., Kangas, A. T., Pakkasjarvi, L., Jaatinen, R. & Thesleff, I. 2003. Stimulation of ectodermal organ development by Ectodysplasin-A1. *Dev Biol,* 259**,** 123-36.

Narhi, K., Tummers, M., Ahtiainen, L., Itoh, N., Thesleff, I. & Mikkola, M. L. 2012. Sostdc1 defines the size and number of skin appendage placodes. *Dev Biol,* 364**,** 149-61.

Nelson, C. M. 2016. On Buckling Morphogenesis. *J Biomech Eng,* 138**,** 021005.

Nguyen-Ngoc, K. V., Silvestri, V. L., Georgess, D., Fairchild, A. N. & Ewald, A. J. 2017. Mosaic loss of non-muscle myosin IIA and IIB is sufficient to induce mammary epithelial proliferation. *J Cell Sci,* 130**,** 3213-3221.

Nusse, R. & Clevers, H. 2017. Wnt/beta-Catenin Signaling, Disease, and Emerging Therapeutic Modalities. *Cell,* 169**,** 985-999.

Nusslein-Volhard, C. & Wieschaus, E. 1980. Mutations affecting segment number and polarity in Drosophila. *Nature,* 287**,** 795-801.

Oftedal, O. T. 2002. The mammary gland and its origin during synapsid evolution. *J Mammary Gland Biol Neoplasia,* 7**,** 225-52.

Oftedal, O. T. 2012. The evolution of milk secretion and its ancient origins. *Animal,* 6**,** 355-68.

Oftedal, O. T. & Dhouailly, D. 2013. Evo-devo of the mammary gland. *J Mammary Gland Biol Neoplasia,* 18**,** 105-20.

Ornitz, D. M. & Itoh, N. 2015. The Fibroblast Growth Factor signaling pathway. *Wiley Interdiscip Rev Dev Biol,* 4**,** 215-66.

Ouspenskaia, T., Matos, I., Mertz, A. F., Fiore, V. F. & Fuchs, E. 2016. WNT-SHH Antagonism Specifies and Expands Stem Cells prior to Niche Formation. *Cell,* 164**,** 156-169.

Paine, I. S. & Lewis, M. T. 2017. The Terminal End Bud: the Little Engine that Could. *J Mammary Gland Biol Neoplasia,* 22**,** 93-108.

Painter, K. J., Hunt, G. S., Wells, K. L., Johansson, J. A. & Headon, D. J. 2012. Towards an integrated experimental-theoretical approach for assessing the mechanistic basis of hair and feather morphogenesis. *Interface Focus,* 2**,** 433-50.

Panagi, M., Voutouri, C., Mpekris, F., Papageorgis, P., Martin, M. R., Martin, J. D., Demetriou, P., Pierides, C., Polydorou, C., Stylianou, A., Louca, M., Koumas, L., Costeas, P., Kataoka, K., Cabral, H. & Stylianopoulos, T. 2020. TGF-beta inhibition combined with cytotoxic nanomedicine normalizes triple negative breast cancer microenvironment towards anti-tumor immunity. *Theranostics,* 10**,** 1910-1922.

Panchal, H., Wansbury, O., Parry, S., Ashworth, A. & Howard, B. 2007. Neuregulin3 alters cell fate in the epidermis and mammary gland. *BMC Dev Biol,* 7**,** 105.

Panousopoulou, E. & Green, J. B. 2016. Invagination of Ectodermal Placodes Is Driven by Cell Intercalation-Mediated Contraction of the Suprabasal Tissue Canopy. *PLoS Biol,* 14**,** e1002405.

Parmar, H. & Cunha, G. R. 2004. Epithelial-stromal interactions in the mouse and human mammary gland in vivo. *Endocr Relat Cancer,* 11**,** 437-58.

Perez-Vale, K. Z. & Peifer, M. 2020. Orchestrating morphogenesis: building the body plan by cell shape changes and movements. *Development,* 147.

Pilot, F. & Lecuit, T. 2005. Compartmentalized morphogenesis in epithelia: from cell to tissue shape. *Dev Dyn,* 232**,** 685-94.

Pispa, J., Mustonen, T., Mikkola, M. L., Kangas, A. T., Koppinen, P., Lukinmaa, P. L., Jernvall, J. & Thesleff, I. 2004. Tooth patterning and enamel formation can be manipulated by misexpression of TNF receptor Edar. *Dev Dyn,* 231**,** 432-40.

Pispa, J. & Thesleff, I. 2003. Mechanisms of ectodermal organogenesis. *Dev Biol,* 262**,** 195-205.

Pond, C. M. 1977. The Significance of Lactation in the Evolution of Mammals. *Evolution,* 31**,** 177-199.

Prevot, V. 2015. Puberty in mice and rats. *Knobil and Neill's physiology of reproduction. New York: Elsevier***,** 1395-439.

Propper, A. 1968. Relationsé pidermo-mésodermiques dans la diffé renciation de l'ébauche mammaire d'embryon de lapin.: Annals of Embryology and Morphology.

Propper, A. & Gomot, L. 1967. Interactions tissulaires au cours de l'organogenèse de la glande mammaire de l'embryon de lapin. Comptes Rendus de l'Académie des Sciences (Paris).

Propper, A. & Gomot, L. 1973. Control of chick epidermis differentiation by rabbit mammary mesenchyme. *Experientia,* 29**,** 1543-4.

Propper, A. Y. 1973. *Contribution à l'étude du développement embryonnaire*

de la glande mammaire chez le lapin (Oryctolagus Cuniculus L.). Université de Besançon.

Propper, A. Y. 1978. Wandering epithelial cells in the rabbit embryo milk line. A preliminary scanning electron microscope study. *Dev Biol,* 67**,** 225-31.

Propper, A. Y., Howard, B. A. & Veltmaat, J. M. 2013. Prenatal morphogenesis of mammary glands in mouse and rabbit. *J Mammary Gland Biol Neoplasia,* 18**,** 93-104.

Rajaram, R. D., Buric, D., Caikovski, M., Ayyanan, A., Rougemont, J., Shan, J., Vainio, S. J., Yalcin-Ozuysal, O. & Brisken, C. 2015. Progesterone and Wnt4 control mammary stem cells via myoepithelial crosstalk. *EMBO J,* 34**,** 641-52.

Reyes-Reali, J., Mendoza-Ramos, M. I., Garrido-Guerrero, E., Mendez-Catala, C. F., Mendez-Cruz, A. R. & Pozo-Molina, G. 2018. Hypohidrotic ectodermal dysplasia: clinical and molecular review. *Int J Dermatol,* 57**,** 965-972.

Richardson, R. J., Hammond, N. L., Coulombe, P. A., Saloranta, C., Nousiainen, H. O., Salonen, R., Berry, A., Hanley, N., Headon, D., Karikoski, R. & Dixon, M. J. 2014. Periderm prevents pathological epithelial adhesions during embryogenesis. *J Clin Invest,* 124**,** 3891-900.

Riddihough, G. & Ish-Horowicz, D. 1991. Individual stripe regulatory elements in the Drosophila hairy promoter respond to maternal, gap, and pair-rule genes. *Genes Dev,* 5**,** 840-54.

Robinson, G. W., Karpf, A. B. & Kratochwil, K. 1999. Regulation of mammary gland development by tissue interaction. *J Mammary Gland Biol Neoplasia,* 4**,** 9-19.

Rohrschneider, L. R., Custodio, J. M., Anderson, T. A., Miller, C. P. & Gu, H. 2005. The intron 5/6 promoter region of the ship1 gene regulates expression in stem/progenitor cells of the mouse embryo. *Dev Biol,* 283**,** 503-21.

Ruan, W. & Kleinberg, D. L. 1999. Insulin-like growth factor I is essential for terminal end bud formation and ductal morphogenesis during mammary development. *Endocrinology,* 140**,** 5075-81.

Sadier, A., Viriot, L., Pantalacci, S. & Laudet, V. 2014. The ectodysplasin pathway: from diseases to adaptations. *Trends Genet,* 30**,** 24-31.

Sakakura, T. 1987. The mammary gland: development, regulation, and function. *Mammary Embryogenesis. Plenum Press, New York***,** 37-66.

Sakakura, T., Nishizuka, Y. & Dawe, C. J. 1976. Mesenchyme-dependent morphogenesis and epithelium-specific cytodifferentiation in mouse mammary gland. *Science,* 194**,** 1439-41.

Sakakura, T., Sakagami, Y. & Nishizuka, Y. 1982. Dual origin of mesenchymal tissues participating in mouse mammary gland embryogenesis. *Dev Biol,* 91**,** 202-7.

Sakaue-Sawano, A., Kurokawa, H., Morimura, T., Hanyu, A., Hama, H., Osawa, H., Kashiwagi, S., Fukami, K., Miyata, T., Miyoshi, H., Imamura, T., Ogawa, M., Masai, H. & Miyawaki, A. 2008. Visualizing spatiotemporal dynamics of multicellular cell-cycle progression. *Cell,* 132**,** 487-98.

Satokata, I., Ma, L., Ohshima, H., Bei, M., Woo, I., Nishizawa, K., Maeda, T., Takano, Y., Uchiyama, M., Heaney, S., Peters, H., Tang, Z., Maxson, R. & Maas, R. 2000. Msx2 deficiency in mice causes pleiotropic defects in bone growth and ectodermal organ formation. *Nat Genet,* 24**,** 391-5.

Schmidt-Ullrich, R., Aebischer, T., Hulsken, J., Birchmeier, W., Klemm, U. & Scheidereit, C. 2001. Requirement of NF-kappaB/Rel for the development of hair follicles and other epidermal appendices. *Development,* 128**,** 3843-53.

Schock, F. & Perrimon, N. 2002. Molecular mechanisms of epithelial morphogenesis. *Annu Rev Cell Dev Biol,* 18**,** 463-93.

Sengel, P. 1976. Morphogenesis of skin. *Developmental and cell biology series***,** 1-17.

Shindo, A. 2018. Models of convergent extension during morphogenesis. *Wiley Interdiscip Rev Dev Biol,* 7.

Shioi, G., Kiyonari, H., Abe, T., Nakao, K., Fujimori, T., Jang, C. W., Huang, C. C., Akiyama, H., Behringer, R. R. & Aizawa, S. 2011. A mouse reporter line to conditionally mark nuclei and cell membranes for in vivo live-imaging. *Genesis,* 49**,** 570-8.

Shutova, M. S., Spessott, W. A., Giraudo, C. G. & Svitkina, T. 2014. Endogenous species of mammalian nonmuscle myosin IIA and IIB include activated monomers and heteropolymers. *Curr Biol,* 24**,** 1958-68.

Shutova, M. S. & Svitkina, T. M. 2018. Common and Specific Functions of Nonmuscle Myosin II Paralogs in Cells. *Biochemistry (Mosc),* 83**,** 1459-1468.

Sick, S., Reinker, S., Timmer, J. & Schlake, T. 2006. WNT and DKK determine hair follicle spacing through a reaction-diffusion mechanism. *Science,* 314**,** 1447-50.

Small, S., Kraut, R., Hoey, T., Warrior, R. & Levine, M. 1991. Transcriptional regulation of a pair-rule stripe in Drosophila. *Genes Dev,* 5**,** 827-39.

Srivastava, A. K., Pispa, J., Hartung, A. J., Du, Y., Ezer, S., Jenks, T., Shimada, T., Pekkanen, M., Mikkola, M. L., Ko, M. S., Thesleff, I., Kere, J. & Schlessinger, D. 1997. The Tabby phenotype is caused by mutation in a mouse homologue of the EDA gene that reveals novel mouse and human exons and encodes a protein (ectodysplasin-A) with collagenous domains. *Proc Natl Acad Sci U S A,* 94**,** 13069-74.

Sutkeviciute, I., Clark, L. J., White, A. D., Gardella, T. J. & Vilardaga, J. P. 2019. PTH/PTHrP Receptor Signaling, Allostery, and Structures. *Trends Endocrinol Metab,* 30**,** 860-874.

Travis, A., Amsterdam, A., Belanger, C. & Grosschedl, R. 1991. LEF-1, a gene encoding a lymphoid-specific protein with an HMG domain, regulates T-cell receptor alpha enhancer function [corrected]. *Genes Dev,* 5**,** 880-94.

Turing, A. M. 1952. The chemical basis of morphogenesis. *Phil. Trans. R. Soc. Lond. B,* 237**,** 37–72.

Vaahtokari, A., Aberg, T. & Thesleff, I. 1996. Apoptosis in the developing tooth: association with an embryonic signaling center and suppression by EGF and FGF-4. *Development,* 122**,** 121-9.

Van Der Wal, T. & Van Amerongen, R. 2020. Walking the tight wire between cell adhesion and WNT signalling: a balancing act for beta-catenin. *Open Biol,* 10**,** 200267.

Van Genderen, C., Okamura, R. M., Farinas, I., Quo, R. G., Parslow, T. G., Bruhn, L. & Grosschedl, R. 1994. Development of several organs that require inductive epithelial-mesenchymal interactions is impaired in LEF-1-deficient mice. *Genes Dev,* 8**,** 2691-703.

Veltmaat, J. M., Mailleux, A. A., Thiery, J. P. & Bellusci, S. 2003. Mouse embryonic mammogenesis as a model for the molecular regulation of pattern formation. *Differentiation,* 71**,** 1-17.

Veltmaat, J. M., Relaix, F., Le, L. T., Kratochwil, K., Sala, F. G., Van Veelen, W., Rice, R., Spencer-Dene, B., Mailleux, A. A., Rice, D. P., Thiery, J. P. & Bellusci, S. 2006. Gli3-mediated somitic Fgf10 expression gradients are required for the induction and patterning of mammary epithelium along the embryonic axes. *Development,* 133**,** 2325-35.

Veltmaat, J. M., Van Veelen, W., Thiery, J. P. & Bellusci, S. 2004. Identification of the mammary line in mouse by Wnt10b expression. *Dev Dyn,* 229**,** 349-56.

Voutilainen, M., Lindfors, P. H., Lefebvre, S., Ahtiainen, L., Fliniaux, I., Rysti, E., Murtoniemi, M., Schneider, P., Schmidt-Ullrich, R. & Mikkola, M. L. 2012. Ectodysplasin regulates hormone-independent mammary ductal morphogenesis via NF-kappaB. *Proc Natl Acad Sci U S A,* 109**,** 5744-9.

Voutilainen, M., Lindfors, P. H. & Mikkola, M. L. 2013. Protocol: ex vivo culture of mouse embryonic mammary buds. *J Mammary Gland Biol Neoplasia,* 18**,** 239-45.

Wang, J. & Shackleford, G. M. 1996. Murine Wnt10a and Wnt10b: cloning and expression in developing limbs, face and skin of embryos and in adults. *Oncogene,* 13**,** 1537-44.

Wang, Q. A. & Scherer, P. E. 2019. Remodeling of Murine Mammary Adipose Tissue during Pregnancy, Lactation, and Involution. *J Mammary Gland Biol Neoplasia,* 24**,** 207-212.

Wang, Y., Dong, J., Li, D., Lai, L., Siwko, S., Li, Y. & Liu, M. 2013. Lgr4 regulates mammary gland development and stem cell activity through the pluripotency transcription factor Sox2. *Stem Cells,* 31**,** 1921-31.

Wansbury, O., Panchal, H., James, M., Parry, S., Ashworth, A. & Howard, B. 2008. Dynamic expression of Erbb pathway members during early mammary gland morphogenesis. *J Invest Dermatol,* 128**,** 1009-21.

Watson, C. J. & Khaled, W. T. 2020. Mammary development in the embryo and adult: new insights into the journey of morphogenesis and commitment. *Development,* 147.

Wee, P. & Wang, Z. 2017. Epidermal Growth Factor Receptor Cell Proliferation Signaling Pathways. *Cancers (Basel),* 9.

Wiese, K. E., Nusse, R. & Van Amerongen, R. 2018. Wnt signalling: conquering complexity. *Development,* 145.

Williams, J. M. & Daniel, C. W. 1983. Mammary ductal elongation: differentiation of myoepithelium and basal lamina during branching morphogenesis. *Dev Biol,* 97**,** 274-90.

Wilson, K. J., Mill, C., Lambert, S., Buchman, J., Wilson, T. R., Hernandez-Gordillo, V., Gallo, R. M., Ades, L. M., Settleman, J. & Riese, D. J., 2nd 2012. EGFR ligands exhibit functional differences in models of paracrine and autocrine signaling. *Growth Factors,* 30**,** 107-16.

Wilson, W. K. & Dudley, F. 1952. The duration of gestation in rabbit breeds and crosses. *Journal of Genetics,* 50**,** 384.

Wolpert, L. 1969. Positional information and the spatial pattern of cellular differentiation. *J Theor Biol,* 25**,** 1-47.

Wolpert, L. 1971. Positional information and pattern formation. *Curr Top Dev Biol,* 6**,** 183-224.

Wright, J. T., Fete, M., Schneider, H., Zinser, M., Koster, M. I., Clarke, A. J., Hadj-Rabia, S., Tadini, G., Pagnan, N., Visinoni, A. F., Bergendal, B., Abbott, B., Fete, T., Stanford, C., Butcher, C., D'souza, R. N., Sybert, V. P. & Morasso, M. I. 2019. Ectodermal dysplasias: Classification and organization by phenotype, genotype and molecular pathway. *Am J Med Genet A,* 179**,** 442-447.

Wysolmerski, J. J., Philbrick, W. M., Dunbar, M. E., Lanske, B., Kronenberg, H. & Broadus, A. E. 1998. Rescue of the parathyroid hormone-related protein knockout mouse demonstrates that parathyroid hormone-related protein is essential for mammary gland development. *Development,* 125**,** 1285-94.

Xie, Y., Su, N., Yang, J., Tan, Q., Huang, S., Jin, M., Ni, Z., Zhang, B., Zhang, D., Luo, F., Chen, H., Sun, X., Feng, J. Q., Qi, H. & Chen, L. 2020. FGF/FGFR signaling in health and disease. *Signal Transduct Target Ther,* 5**,** 181.

Yan, M., Zhang, Z., Brady, J. R., Schilbach, S., Fairbrother, W. J. & Dixit, V. M. 2002. Identification of a novel death domain-containing adaptor molecule for ectodysplasin-A receptor that is mutated in crinkled mice. *Curr Biol,* 12**,** 409-13.

Yu, M., Zhan, J. & Zhang, H. 2020. HOX family transcription factors: Related signaling pathways and post-translational modifications in cancer. *Cell Signal,* 66**,** 109469.

Zhang, X., Ibrahimi, O. A., Olsen, S. K., Umemori, H., Mohammadi, M. & Ornitz, D. M. 2006. Receptor specificity of the fibroblast growth factor family. The complete mammalian FGF family. *J Biol Chem,* 281**,** 15694-700.

Zhang, Y., Tomann, P., Andl, T., Gallant, N. M., Huelsken, J., Jerchow, B., Birchmeier, W., Paus, R., Piccolo, S., Mikkola, M. L., Morrisey, E. E., Overbeek, P. A., Scheidereit, C., Millar, S. E. & Schmidt-Ullrich, R. 2009. Reciprocal requirements for EDA/EDAR/NF-kappaB and Wnt/beta-catenin signaling pathways in hair follicle induction. *Dev Cell,* 17**,** 49-61.